YTUP

Journal of Thermal Engineering
https://jten.yildiz.edu.tr/
https://doi.org/10.47481/jten.0022

REVIEW ARTICLE

# Recent advances in single-phase liquid cooling techniques for performance enhancement of microchannel heat sinks: a review

K. Bala Subrahmanyam[1,*], Valaparla Ranjith Kumar[2], Pritam Das[3], G.R.K. Sastry[4], Sameer S. Gajghate[5]

[1]Associate Professor, Department of Mechanical Engineering, Sri Vasavi Engineering College, Pedatadepalli, Tadepalligudem, Andhra Pradesh, 534101, India
[2]Associate Professor, Department of Mechanical Engineering, Vignan's Institute of Information Technology, Duvvada, Vizag, 530049, India
[3]Associate Professor, Department of Mechanical Engineering, National Institute of Technology Agartala, Agartala, Tripura, 799046, India
[4]Professor, Department of Mechanical Engineering, National Institute of Technology Andhra Pradesh, Tadepalligudem, Andhra Pradesh, 534101, India
[5]Assistant Professor, Department of Mechanical Engineering, G H Raisoni College of Engineering & Management, Pune, Maharashtra, 412207, India

## Abstract

Rapid advancements in electronic technologies have resulted in progressively higher heat flux in electronic devices installed in high-power integrated circuit packages (microchips) over time. Consequently, thermal management has become a critical issue across industrial sectors, therefore, it is important to explore new methods to improve the reliability, meet demand and extend chip lifetime. Microchannel heat sinks (MCHS) have become a highly promising solution for single-phase liquid cooling, necessitating a comprehensive assessment their current state of development. This review steered by emerging quality and standardized exploration in microchannels and different operating parameters, and is extended with the latest studies. The primary objective of this study is to review the experimental, and numerical results, and key aspects of existing liquid cooling systems, with emphasis placed on frictional behaviour, convective heat transfer characteristics, and operational parameters influencing microchannel performance. The study aims to extend the current cooling methodologies, such as hybrid nanofluids, exploiting thermophysical properties and by integrating secondary channels. The Hybrid nano/monofluids at different volume concentrations have considerable potential working fluids for heat transport. This review consolidates recent progress in experimental practices, numerical modelling of microchannel heat sinks (MCHS), and the applicability of MCHS to single-phase active cooling techniques. It covers various heat transfer mechanisms, including structural design advancements, substrate materials, working fluids such as nanofluids with different chemical combinations and proportions synthesized to improve properties, operating conditions in terms of Reynolds number and the quantitative role of the latest optimization algorithms. Significant progress has been reported in the recent development of geometric modifications, includingribs, cavities and secondary channels, with fully developed flow models and developing flow contributes to a appreciate temperature decrease which enhance heat transfer, maximum reduction in thermal resistance. These advances also identify future opportunities for achieving greater design freedom brought by advanced manufacturing techniques to improve single-phase active cooling systems.

**Keywords:** Microchannel heat sink (mchs), developing flow, fully developed flow, rectangular channels, forced convection, ribs and cavities, nanofluids

**Cite this article as:** Subrahmanyam, K. B., Kumar, V. R., Das, P., Sastry, G. R. K., & Gajghate, S. S. (2026). Recent advances in single-phase liquid cooling techniques for performance enhancement of microchannel heat sinks: A review. Journal of Thermal Engineering, 12(3), 1172–1195. https://doi.org/10.47481/jten.0022

*Corresponding Author
E-mail Adress: kbsm0009@gmail.com

**Submitted:** 9 February 2025; **Accepted:** 24 December 2025

This paper was recommended for publication in revised form by Editorin-Chief Ahmet Selim Dalkılıç

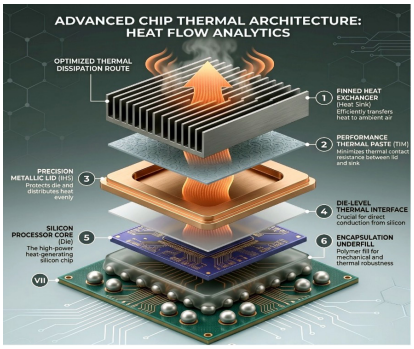


**Figure 1.** Microchannel design characteristics – Thermal management architectures

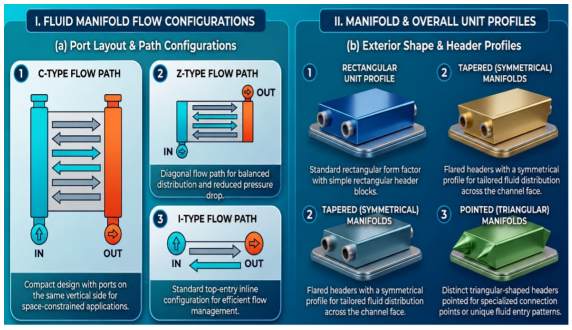


**Figure 2.** (a) Schematic diagram of different inlet/outlet locations and (b) Header designs of heat sinks

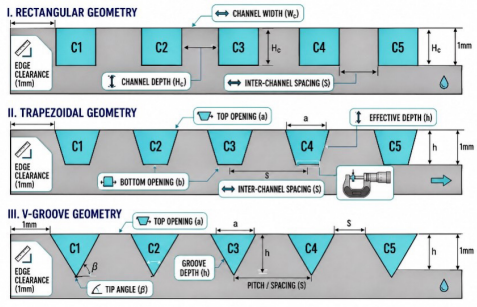


**Figure 3.** Illustration of different shapes of heat sink sections with its dimensions

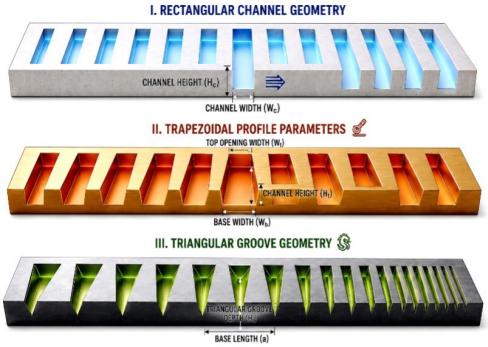


**Figure 4.** Illustration of Cross section of different heat sinks with its dimensions

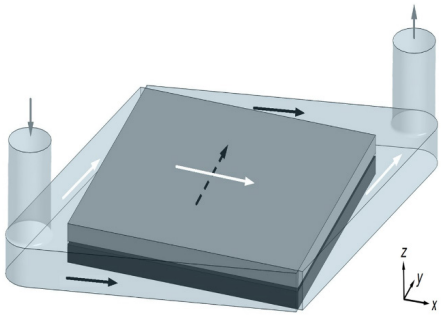


**Figure 5.** A crossflow - crossflow averaged overall geometry, including headers, by Savino et al. [18]

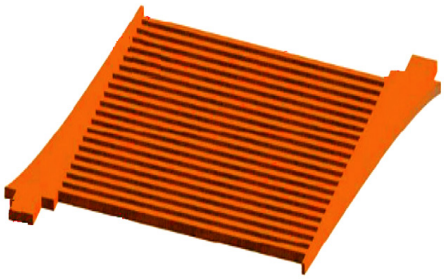

**Figure 6.** Velocity field of the optimized design inlet headers by shao et al. [19]

## 1. Introduction

The increasing usage of high-heat-flux systems and advances in electronic technology have tremendously increased transistor density, resulting in integrated circuits that increase heat dissipation and pose significant challenges to improving heat transfer efficiency. Various conventional heat-transfer augmentation techniques such as jet impingement, and spray cooling coolant flows, lead to high energy consumption to carry away the heat flux and also require more open space for a consistent cooling effect. However, conventional MCHS have drawbacks, including excessive wall overheating, burnout, high pressure drop, and inconsistent temperature distribution. In light of the above problems, researchers immersed themselves in the design and upgrading of MCHS to advance thermal performance, in the past few years. Compared with conventional pipe flows, liquid-cooled MCHS is an efficient, cost-competitive solution that offers promising heat transfer capacity, flow regime that results in a high surface area-to-volume ratio, enhanced temperature uniformity, and a compact design, thereby attracting significant attention from researchers.

In the present work, a large number of experimental and numerical investigations were undertaken on single-phase active cooling of smooth, rectangular, and various channel-geometry combinations. The development in the field of MCHS flow-disruption mechanisms promoted by designs such as ribs/fins and cavities/grooves, and by hybrid cooling techniques including secondary channels,

jet impingement, double-layered configurations, and Nanofluids heat-transfer enhancement has been discussed. Moreover, the focus is on how design advancements and operating parameters that are intimately involved in flow mixing led to significant improvements in heat transfer performance; these are discussed in detail. Tuckerman and Pease et al. [1] first instigated the application of miniaturization experimentally on rectangular MCHS. They proposed a high-performance heat sink, which plays a vital role in fulfilling the requirement of a highly efficient and accurate compact heat exchanger that can handle heat dissipation of 790 W/cm$^2$ for high-speed VLSI circuits. Webb et al. [2] proposed four heat transfer enhancement methods and established equations for performance evaluation criteria (PEC) for heat exchanger optimum performance evaluation, till today those equations are still in use. However, the extensive work conducted on an effective heat transfer assessment method has provided motivation, used by many authors. Steinke and Kandlikar et al. [3] summarized review of available studies regarding single-phase heat transfer enhancement techniques, elaborated active and passive methods. They covered heat transfer augmentation techniques including flow transition, breakup of the boundary layer, entrance-region techniques, vibration, electric fields, and swirl flow, and proposed new cross-mixing designs between two adjacent liquid streams. They also proposed various methods for generating secondary flows by introducing smaller channels between the main flow channels. They made the initial, conventional MCHS heat-transfer analysis more concrete.

Kroeker et al. [4] provided a more specific review on validity of the continuum model approach for solving three-dimensional conjugate heat transfer problems. They observed that numerical results of fluid flow and heat transfer generated by the continuum model matched very well with the experimental results at the micro-scale. Based on the analysis, they identified that the optimal fin thickness depends on height, material conductivity, and the thermo-physical properties of the fluid. However, it is independent of pumping power, fluid viscosity, and the channel length. Prasher et al. [5] reviewed progress rheology-based modelling and design of polymeric material usage, focused on thermal solutions in developing microelectronics. Their review of the progress made in this area are applications of nanoparticles, nanotubes, and polymeric (thermal interface) materials for its reliability in performance. Thermal architecture typically used in desktop is depicted in Figure 1. They focused on the phenomenon of minimizing thermal resistance between chip surfaces and substrates. Historically, they have compared rheological modelling with the dependence of bulk thermal resistance on particle volume fraction. They identified the importance of minimizing thermal resistance rather than increasing thermal conductivity. Experimental and numerical studies of thermal performance in MCHS with single-phase, laminar flow are summarized in Table 1.

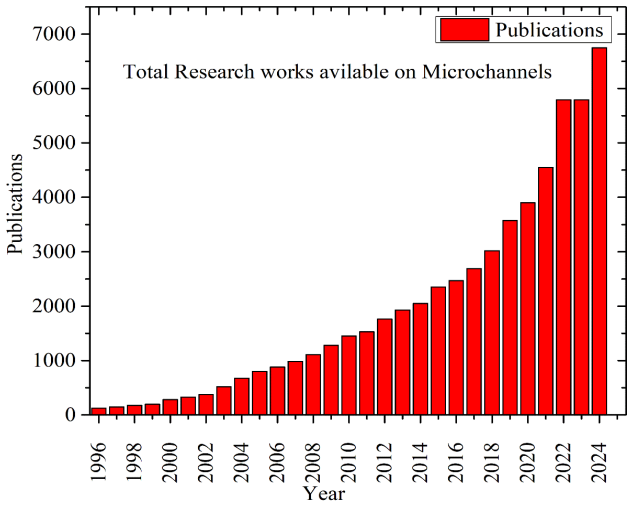


**Figure 7.** Scholarly literature available globally in the area of MCHS from 1996 to 2024 in Google Scholar

Mahalingam et al. [6] performed experimental studies on silicon substrates with non-compressible flow (water) and compressible flow (air). They identified that thermal resistance depends on power dissipation and on flow rates, and velocities of water. Their experimental results revealed that at different flow rates of 12 cm$^3$/s, 63 cm$^3$/s, and the thermal resistances are 0.03 K/W, 0.02 K/W, respectively; corresponding heat removal rates are 2.4 W/cm$^2$, 3.6 W/cm$^2$, respectively.

Kishimoto and Osaki et al. [7] developed high-density stack packaging to increase volume power density for multichip packaging applications at lower thermal resistance. To identify it, they designed and fabricated an alumina substrate with a cross section of 800 μm

wide x 400 μm high. The experimental study reveals optimal structure dimensions for cooling, and identifies that cooling capability depends on uniform coolant flow distribution. However, they also fabricated an indirect liquid cooling package to mount VLSI chips above multi-layered substrates, the heat dissipation was higher than 400 Watts per package at a flow rate of 1.0 litre/min. Phillips et al. [8] extended the theoretical analysis done by Tuckerman and Pease [1]. They focused on small, moderate, and large channel aspect ratios for developing and fully developed flows in laminar and turbulent regimes. They investigated the characteristics of smooth, and roughened (with repeated ribs) surfaces, finding a pressure drop of 414 kPa and the lowest thermal resistance of 0.072 K/W. Their study noted that variation in the Nusselt number is attributable to the coolant phase, properties, flow rate, flow regime (laminar, transition, and turbulent), channel geometry, axial position, and heat input boundary conditions. Harpole et al. [9] developed numerical model of the multi-dimensional flow model, designed silicon etched manifold system that forces liquid flow between the fins and focused on optimizing design parameters. The experimental evaluations revealed that the favorable scaling of increments in geometrical dimensions and decrements in flow rate depends on heat flux. Furthermore,

the investigation indicates that the optimum fin thickness should be half of the channel width, which can reduce flow resistance with increased fluid flow area and achieved heat transfer coefficient of 100 W/cm$^2$K at a pressure drop of 2 bar.

Figure 7 shows the scientific platform Google scholar, which clearly exhibits using data from research articles published from 1996 to 2024. A gradual growth trend in MCHS research has been observed over the years. The growth of computer applications has driven a substantial demand for low power consumption and improved thermal performance, attracting the focus of traditional researchers toward further design advancements. Throughout the study, they observed that the pressure drop was the major drawback of MCHS flows.

**Table 1.** A summary of selected literature based on geometry of ribs, cavities and secondary channels for comparative study in MCHS based on thermal performance (TP)

| Authors | Configuration | Parameter ranges, Substrate material and heat flux | Observations and Limitations |
|---|---|---|---|
| Kuppusa my et al. [12] | Triangular grooved MCHS | geometrical parameters ranges are the grove angle (50–100$^0$), depth (10–25 μm) and pitch (400–550 μm), Re = 266.12, 532.24, and 798.36, with a heat flux of $10^6$ W/m$^2$ | The best geometrical parameters identified for triangular cavity model observed at angle of groove, depth of groove, pitch are 100$^0$, 25 μm and 450 μm, respectively and Nusselt number, efficiency is increased by 189.84%, 179.55% respectively. |
| Xia et al. [17] | Header shapes (triangular, trapezoidal and rectangular), inlet/outlet locations (I, C and Z-type) | Hydraulic diameter is 0.15 mm, and the aspect ratio is 0.333, fluid flow rate increases from 100 ml/min to 200 ml/min, with a heat flux of 200 W/cm$^2$ | Compared MCHS with offset fan-shaped re-entrant cavities and triangular re-entrant cavities), identified lower pressure drop, bottom wall temperature for triangular re-entrant cavities at fluid flow rate of 150 ml/min with I-type. |
| Savino et al. [18] | Double layered cross flow, header design | Height, width and length equal to 0.5, 0.1 and 10 mm, cases are with baffle, without baffle, cut baffle, porous baffle with a heat flux of 100 W/cm$^2$, Re ≤ 1000 | Thermal resistance was reduced by 11.8%, 7.1%, and 4.4% compared to the case with uniform inlet velocities for average MCHS velocities equal to 0.5, 1, and 2 m/s, respectively. |
| Shao et al. [19] | Inlet header design | MCHS with cross-sectional size of each 0.5 mm × 0.5 mm, 20 channels, inlet velocities considered from 0.05 to 0.1 m/sec, with a heat flux of 7.9 MW/m$^2$ | Structural optimization done based on surrogate model combined with genetic algorithm, for the inlet velocity of 0.05 to 0.1 m/s, optimal inlet header design reduces non-uniformity by 52.43% to 33.17% respectively, compared with original design. |
| Chai et al. [24] | Ribs including rectangular, backward triangular, isosceles triangular, forward triangular and semicircular on side walls | Geometrical parameters of rib width of 0.05 mm, height 0.025 mm, 190 ≤ Re ≤ 838 Silicon, with a heat flux of $10^6$ W/m$^2$ | MCHS with new ribs design proposed yield Nusselt number of 1.42–1.95 and apparent friction factor of 1.93–4.57 times higher than the smooth channel which leads to performance evaluation criteria of 1.02–1.48. |
| Chai et al. [25] | Aligned and offset fan-shaped ribs on sidewalls | Geometrical parameters of rib width (0.05–0.4 mm), height (0.005–0.025 mm) and spacing (0.2–5 mm) 187< Re <715, Silicon, with a heat flux of $10^6$ W/m$^2$ | Average Nusselt number increment of 6 - 101%, a decrement in thermal resistance of 3- 40% with aligned-fan shape rib arrangement, comparatively lower than offset rib arrangement |
| Kuppusa my et al. [55] | Trapezoidal grooved MCHS | Groove widths variation of model a is 40 to 80 μm, model b is 80 to 100 μm, 266.12< Re <798.36, Silicon, with a heat flux of $10^6$ W/m$^2$ | Found that a at 40 μm, b at 100 μm, increasing number of grooves are giving optimum performance. |

| | | | |
|---|---|---|---|
| Ghani et al. [35] | Secondary oblique channels in alternating directions and rectangular ribs | Relative rib width β varies from 0.3 to 0.6, relative secondary channel width from 0.33 to 1.2 and angle θ changes from to 45 to $90^0$, 100 < Re < 500, Copper, with a heat flux of 100 $W/cm^2$ | The best overall performance of 1.98 at Re = 500, Nusselt number exhibits higher values at relative rib width at λ= 0.33 of Re from 100 to 300, at λ= 0.66 of Re above 300. |
| Japar et al. [38] | Triangular cavity and rectangular rib along the secondary channel | Cavity width = 20 μm, secondary channel angle = $30^0$, 100 < Re < 450, Copper, heat flux of 100 $W/cm^2$ | The secondary channel design that connects two main channels has enhanced thermal performance by a maximum of 1.65 at Re = 450 |
| Bahiraei et al. [56] | Hybrid nanofluid flow in MCHS equipped with secondary channels and ribs | Channel length = 10 mm, width = 0.6 mm and height of heat sink = 0.4 mm, 100 < Re < 500, Copper, heat flux of 105 $W/m^2$. | The secondary channel design increases heat transfer surface area, decreases pressure drop and observed a bottom surface temperature of 13.88 K with an increase in Re from 100 to 500. |
| Shi et al. [37] | MCHS with secondary flow channel | Channel length is 10 mm, width of secondary channel from 0.1 to 0.2 mm and secondary channel angle 26.6 to $45^0$, 300 < Re < 1200, Silicon, heat flux of 100 $W/cm^2$. | When the secondary channel width α parameter increases from 1 to 2, it leads to a decrease in pump power by 13.7% and an increase in thermal resistance by 17.2%. This change has a significant impact. |
| Bala Subrahm anyam et al. [38] | MCHS with fan-shaped cavities along with rectangular (RR), backward triangular (BTR), forward triangular (FTR) and diamond (DR) | Geometrical parameters considered Relative width of cavity α (0.40-0.75), Relative length of cavity β (0.025-0.055), Relative width of the rib γ (0.65-1.25), Relative pitch λ (0.0454-0.25), 136 < Re < 588, silicon, with a heat flux of $10^6$ $W/m^2$. | Fan cavity with diamond rib identified are γ=1.25, α=0.75, β= λ= 0.0454, thus highest heat transfer coefficient achieved is 200693.6 $Wm^{-2}K^{-1}$. |

### 1.1. Augmentation techniques

In general, methods for heat transfer enhancement can be classified as passive or active. A major factor in the design of compact heat exchangers is of the selection of passive and active techniques for heat transfer augmentation. In the passive method, no external power input is required, and the power available within the system is used to enhance heat transfer. The recent studies based on conventional passive heat dissipation technology achieved the maximum heat dissipation demand of 1000 $W/cm^2$ by Sharma et al. [10]. However, in the active method, external power input systems are utilized for flow regulation, such as fans, which require an electricity supply to enhance heat transfer and also increase design complexity. Many researchers have made significant improvements in this area using techniques such as fluid vibration, surface vibration, jet impingement, and spray cooling. In the active heat dissipation technology, the manifold design of Z-type has been achieved the ultra-high heat dissipation of 1842 $W/cm^2$ under ultra-low pumping power by Yang et al. [11]. Preliminary mathematical modelling of the Rectangular MCHS

The additional advantage of rectangular-cross-section MCHS has attracted significant attention, facilitating comparative studies and performance evaluations. The design of next-generation electronic devices incorporates multiple functions. The high-speed operations can generate high heat fluxes, that require effective cooling and reliable service. The growth of central processing units (CPUs) in computers and the expansion of their applications have dramatically changed human lifestyles. Because fabricating complex structural 3D geometries is difficult and time-consuming, many researchers have adopted numerical results as evidence to confirm the estimates. However, research and development greatly influence it before it is prepared for production use and priced relatively low.

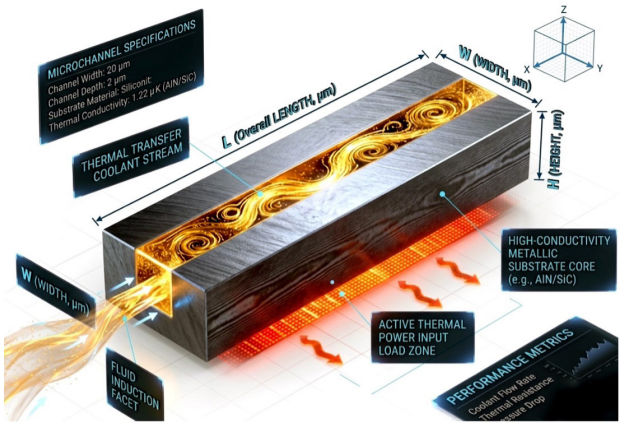


**Figure 8.** Detailed illustration of basic smooth/rectangular MCHS

Figure 8 represents the physical configuration of basic liquid-cooled rectangular MCHS geometry utilized by Kuppusamy et al. [12] as an example, considering that surfaces exposed to the surroundings are insulated except at the bottom surface where constant heat flux is being supplied. The literature survey below describes an organized review of existing research contributions.

### 2.1. Smooth and plain rectangular channels

Design studies of electronic equipment cooling in the 1980s involved forced convection due to fluid flow over (silicon) substrate and conventionally included experimental validation of fully developed laminar flow. Wu and Little et al. [13-14] first conducted an experimental analysis of MCHS heat transfer and frictional resistance characteristics with gas flow. The width and depth varied from 130 to 200 microns and from 30 to 60 microns, respectively. The author recommended using the Sieder-Tate correlation for fully developed laminar flow at Re < 2200. Contrary to conventional theory, they observed that practical friction factors are higher than expected. However, channel wall surface roughness plays a vital role in the early transition from laminar to turbulent flow at Re ranging from 350 to 900.

Peng and Peterson et al. [15-16] experimentally studied the influence of geometric parameters on flow friction and heat transfer characteristics of water flowing through rectangular MCHS made of steel with hydraulic diameters of 0.133-0.367 mm at aspect ratios of H/W = 0.333–1. The author's careful experimental work investigated the transition from laminar to a fully turbulent flow regimes across the Reynolds number range in convective heat transfer. They compared the experimental results with classical theory, and this comparison revealed several new findings. Based on distinct characteristics observed in studies of fluid-flow friction and heat transfer, they found that the Reynolds number ranged from 200 to 700 in laminar flow. Based on the results, they recommended new correlations for the fluid's laminar, and turbulent flows in rectangular MCHS. Their results also indicated a much higher heat transfer coefficient for laminar flow through MCHS than for turbulent flow through conventionally sized channels.

Primary studies are concentrated on convective heat transfer for the most part experimentally on rectangular MCHS by many researchers like Wu and Little et al. [13-14], and Peng et al. [15-16].

## 3. Channel with heat transfer enhancers (flow disruptions)

The principle underlying the chaotic mixing technique has been adopted previously by many researchers. The standard working devices include the simplest low-Reynolds-number cavity flow, which creates mixing. Moreover, mixing efficiency depends on the strategies implemented and can lead to rapid mixing rather than pure diffusion. Xia et al. [17] studied fluid flow and heat transfer characteristics of MCHS numerically. They considered offset fan-shaped, triangular re-entrant cavities with three different inlet/outlet locations (I-, C-, and Z-type) on the side walls, while maintaining even flow distribution, as presented in Figure 2(a). Different header shapes (triangular, trapezoidal, and rectangular) influence flow impingement, as shown in Figure 2(b). They observed that the wall at the header location plays a significant role in fluid distribution, which is associated with static pressure variations and uniform flow velocity along the stream. Savino et al. [18] investigated numerically on double layered cross flow configuration to mitigate hotspots near the outlet port, focused on design of headers that effect into uniform flow velocity distribution to improve heat transfer, as presented in Figure 5. They identified that the proper design of header, and piping is key to a uniform velocity distribution, which ensures a reduction in thermal resistance of up to 11.8% and temperature uniformity. Shao et al. [19] investigated numerically on shape optimization of inlet header in order to maintain uniformity in fluid-flow. To improve the flow distribution characteristics, they used predictions from neural networks combined with a genetic algorithm, the optimized result is presented in Figure 6.

They compared the optimal design with the original design and identified that non-uniformity can be reduced from 52.43% to 33.17% by changing the inlet velocity from 0.05 m/sec to 0.1 m/sec. Lorenz et al. [20] discovered chaos in the form of changing flow patterns oscillation in a regular periodic fashion to irregular, haphazard, and for long periods of time does not appear to repeat their previous path. To study forced dissipative hydrodynamic flow, they formulated nonlinear differential equations and observed the trajectories of their solutions in phase space.

Many studies have investigated the use of MCHS under various flow disruptions. Primary research focuses on the rectangular and circular geometrical parameters of MCHS in terms of aspect ratios and size, and on identifying scaling effects based on convection heat transfer studies. The advancement includes cavity and groove shapes, including triangular, rectangular, trapezoidal, fan-shaped, sinusoidal, transverse microchambers, curvy, wavy, and zigzag forms; rib and fin shapes (including rectangular, forward-triangle, backward-triangle, diamond, elliptic, strip/pin, and oblique fins); and secondary channels as well as interrupted or bifurcated configurations.

Gunnasegaran et al. [21] studied the importance of geometric shapes in heat transfer characteristics, including inlet/outlet ports, wall plenums, and different shapes of rectangular, trapezoidal, and triangular MCHS numerically, as shown in Figure 3. They further identified differences in hydraulic diameter (the combined effect of height and width) on the MCHS heat transfer coefficient. They suggested that rectangular, trapezoidal, and triangular MCHS influence fluid flow and heat transfer behaviour, with MCHS with smaller hydraulic diameters reporting higher maximum heat transfer than circular cross-sectional shapes.

Wang et al. [22] conducted numerical analysis on geometrical parameters, considering different geometric shapes of MCHS. Twelve different aspect ratios for rectangular, MCHS designs, two for trapezoidal designs, and three for designs with a triangular cross-sectional area were also examined, as shown in Figure 4. However, in this study, they have taken the temperature-dependent variation in water viscosity into account. They identified that the numerical prediction bounds of the Navier–Stokes equations and heat transfer theory are fully valid up to a hydraulic diameter of 0.349 mm.

### 3.1. Extended surfaces (fins/ribs), interruptions and bifurcations

Ribs are disruptive wall-mounted structures used extensively to alter the flow pattern, creating flow disturbance by generating excessive swirl, which can significantly enhance heat transfer. However, different rib shapes combined with cavities prevent temperature increases along the flow direction. Previous contributions by different authors also describe symmetric and staggered arrangements along the side walls and central portion of the MCHS. With air as a working fluid, Jubran et al. [23] experimentally investigated the pressure drop characteristics of rectangular modules, focusing on different rib structures like rectangular, triangular, and cylindrical shapes and sizes. They observed that the rectangular rib exhibits a comparatively minimal pressure drop.

Chai et al. [24] conducted a numerical study on the conjugate model and identified the influence of certain variables, such as entrance effects, viscous heating, and temperature-dependent thermophysical properties. They considered offsetting rib designs, including rectangular, backward-triangular, forward-triangular, isosceles-triangular, and semi-circular, at Re from 190 to 838, as represented in Figure 11. They observed that thermal boundary layer thinning enhances mixing as the flow over offset ribs begins to deflect, creating recirculation. Chai et al. [25] numerically investigated aligned, offset fan-shaped rib influence on average Nusselt number and thermal resistance variations. Furthermore, variations in rib width, height, and spacing affect Re, which ranges from 187 to 715. They observed that, with an offset fan-shaped ribs design, the average Nusselt number increased by 4–103% and the total thermal resistance decreased by 2–42% compared with the aligned arrangement, owing to entrance effects. Furthermore, effective convection is observed for arrangements of rib height and spacing, shown as in Figure 9.

Ali et al. [26] performed numerical simulation on V-shaped rib, examined the influence of angle of attack on thermal and hydraulic efficiency. They observed that V-shaped rib at higher angles like $90^0$ significantly producing turbulence, decreases the pressure drop at lower Re values, in contrast at higher Re values at smaller attack angle of $35^0$ producing better heat transfer capabilities at reasonable pressure drop.

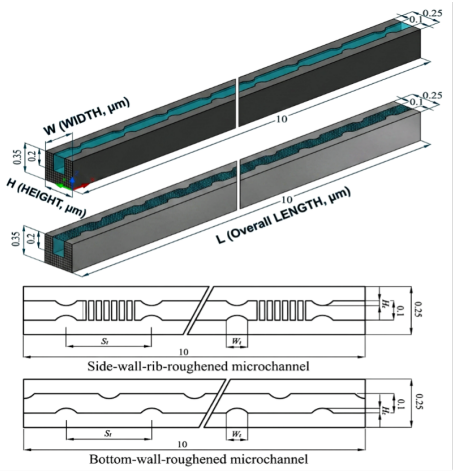


**Figure 9.** Illustration of MCHS design of ribs, cavities and ribs inside cavities – Fan-shaped ribs on side walls

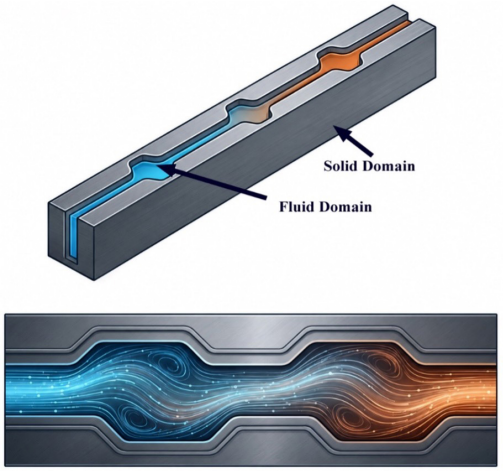


**Figure 10.** Illustration of trapezoidal shaped cavities

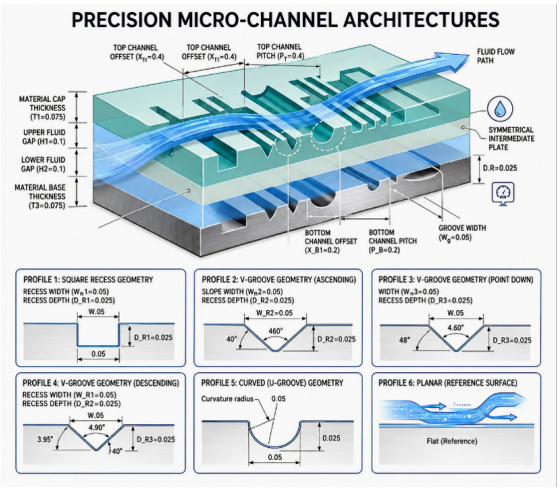


**Figure 11.** Illustration of different shapes of offset ribs

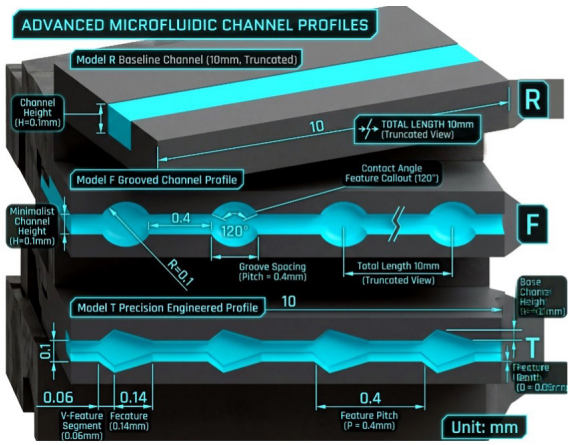


**Figure 12.** Illustration of periodic expansion-constriction (Fan, triangular shaped) cavities

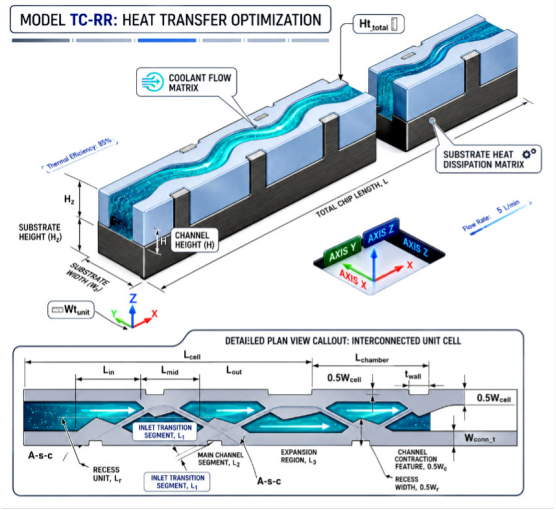


**Figure 13.** Illustration of triangular cavities with rectangular rib (TC-RR)

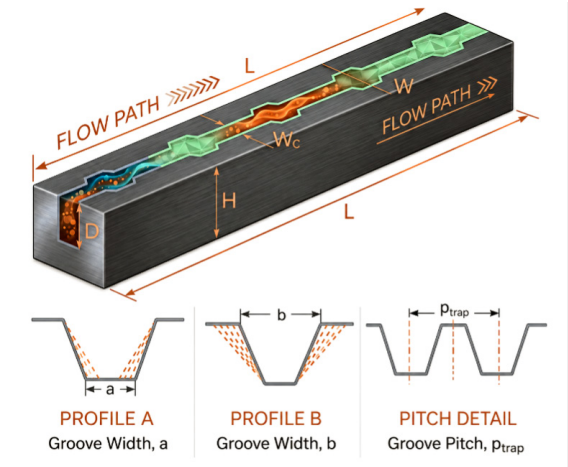


**Figure 14.** Illustration of trapezoidal grooved microchannel heat sink (TGMCHS)

### 3.2. Cavities and grooves

In conventional rectangular MCHS, the thermal entrance effect plays a significant role in the laminar flow regime, identified in many studies using inlet velocity and temperature profiles. However, with variation in scaling effects, aspect ratio, and channel-to-channel spacing as a function of Reynolds number owing to the quantification of coolant flow, has the added benefit. The sudden expansion-constriction/convergent-divergent cross sections, and cavities/grooves, in the entrance lead to a higher heat transfer coefficient because of flow acceleration in the convergent portion caused by developing velocity and temperature profiles. It creates a throttling effect at the throat, whereas this phenomenon creates a jetting effect in the expansion region, and triggers peak velocity near the wall surface. However, these benchmark geometric layouts can noticeably augment heat transfer. Ahmed et al. [27] investigated grooved MCHS heat sinks (GMCHS) by considering geometrical parameters: depth, tip length, pitch, and orientation of cavities for optimization. It was observed that geometric parameters, such as groove-tip length ratio, groove-depth ratio, and the number of grooves markedly influence Nusselt numbers and performance, as presented in Figure 10. They observed higher local Nusselt numbers in the entrance region due to thermally developing flow. Chai et al. [28] performed experimental and numerical studies on MCHS with fan-shaped reentrant cavities, focusing on flow structure and heat transfer characteristics in detail. Ten parallel MCHS had a width of 0.1 mm and a depth of 0.2 mm in constant cross-section segments with fan-shaped (F) reentrant cavities with a field angle of $120^0$, a radius of 0.1 mm and distance between two contiguous cavities of 0.4 mm. The model also includes the expansion-constriction cross-section to study the heat transfer capability, as presented in Figure 12. The design of the re-entrant cavity clearly enhances the heat transfer coefficient, and enables a lower pressure drop at Re < 300, but a drastic increase is observed for 300 < Re < 750, compared with smooth/rectangular channels. Furthermore, they observed that, with increasing pumping power, conductive thermal resistances remain unchanged, whereas convective and capacitive thermal resistances decrease.

Li et al. [29] conducted numerical analysis on the novel triangular cavity rectangular rib (TC-RR) design MCHS, considering relative rib width (α) and relative cavity width (β) parameters to study the heat transfer performance (η). At higher Re, the combined effect of cavity and rib mixing in (TC-RR) is more substantial than in TC and RR and exhibits enhanced heat transfer, as shown in Figure 13. The maximum η = 1.619 is observed at Re = 500, entropy generation number $N_{S,a}$ = 0.5 is observed at Re = 303 with α = 0.3 and β = 2.24. Furthermore, they adopted various cavity and rib shapes.

Ghani et al. [30] conducted a numerical investigation on a proposed new geometry design of the sinusoidal cavity and rectangular ribs to improve heat transfer characteristics. They focused on structural parameters, such as the amplitude and depth of the cavity, rib width, and rib length. The superior hydrothermal performance results from the combined effects of the cavity's large flow area and

the flow disturbances caused by ribs located in the channel's central core. The cooling efficiency varies with channel geometry, such as sinusoidal, wavy, zigzag, and convergent-divergent. Wang et al. [31] investigated numerically on trapezoidal cavity along with front airfoil, rare airfoil rib, rectangular rounded, rectangular rib structures, focused on breaking of thermal boundary layer with increase in Re. They focused on optimizing the design parameters using an artificial neural network based on NSGA-II in order to obtain the highest thermal performance. In a comparison of different rib structures, they identified that the rectangular round rib exhibited the lowest friction coefficient, and the best comprehensive thermal performance (19.3%). Gönül et al. [32] investigated numerically on sinusoidal convergent-divergent along with streamlined pins using multi-objective optimization with Genetic algorithm (NSGA-II). The design parameters considered, amplitudes, wavelengths, and pin heights, are analyzed with respect to Reynolds numbers. The design of streamlined pins produces chaotic advection and secondary flow, significantly improving the performance evaluation criteria (PEC) to 2.23 at minimal pressure drop.

## 4. Hybrid cooling techniques

Advanced hybrid cooling techniques, which incorporate multiple enhancement strategies into a conventional single cooling method, are used to achieve superior heat transfer characteristics such as micro-pin fins, jet impingement, composites, secondary channels with ribs/fins and cavities, phase change materials (PCM), and hybrid manifold design. The integrated cooling method involves complex flow-pattern design that promotes fluid mixing, disrupts thermal boundary layers, and is particularly effective in mitigating localized hot spots to optimize thermal and hydraulic performance. However, these challenges—including fabrication complexities, pressure drop penalties, and the need for advanced optimization of geometry, working fluid, and substrate material properties—are particularly acute for next-generation thermal management solutions which demand high reliability, compactness, and efficient heat dissipation.

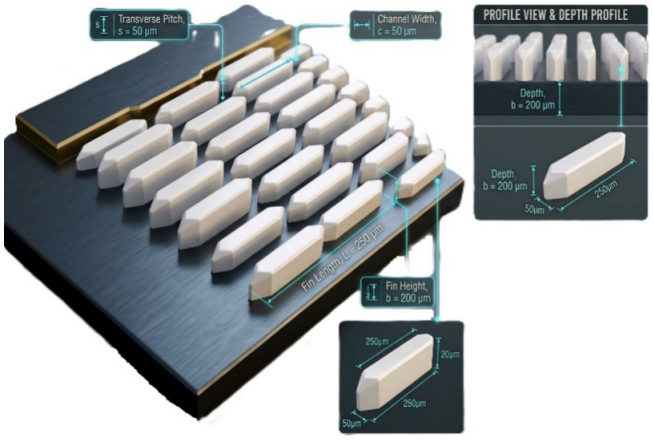


**Figure 15.** Schematic illustration of MCHS designs with secondary channels arrangement – Offset strip fins image of scanning electron microscope (SEC)


**Figure 16.** Illustration of plan view of heat sink with oblique fins

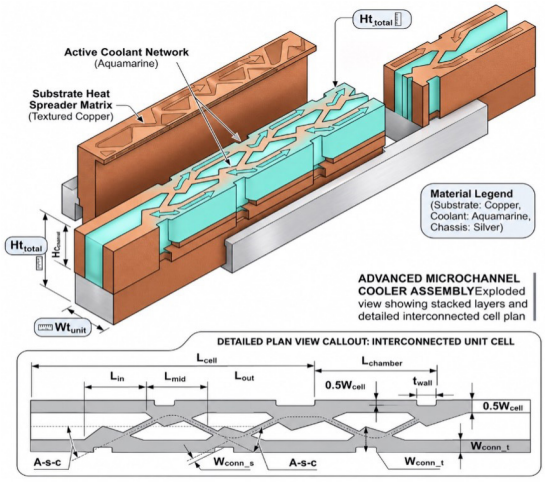


**Figure 17.** Illustration of triangular cavity, rectangular rib and secondary channels (TC-RR-SC)

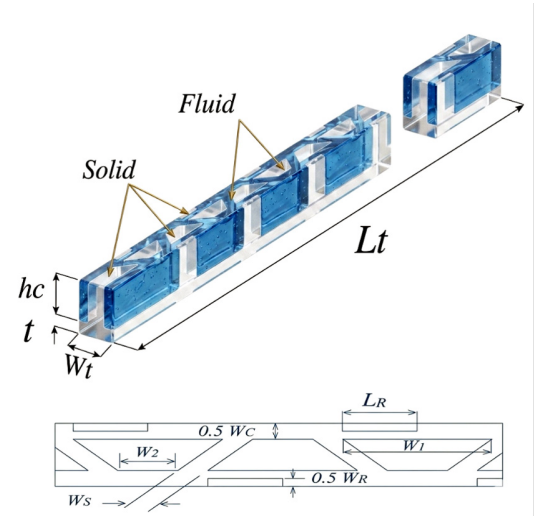


**Figure 18.** Illustration of secondary oblique channels with rectangular rib (MC-SORR)

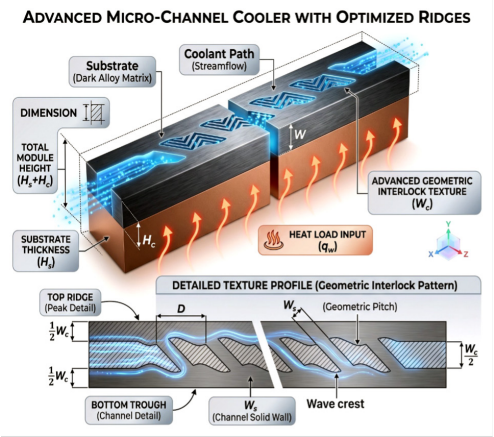


**Figure 19.** Illustration of symmetric wavy MCHS with wave trough-to crest secondary channels (SW-TC)

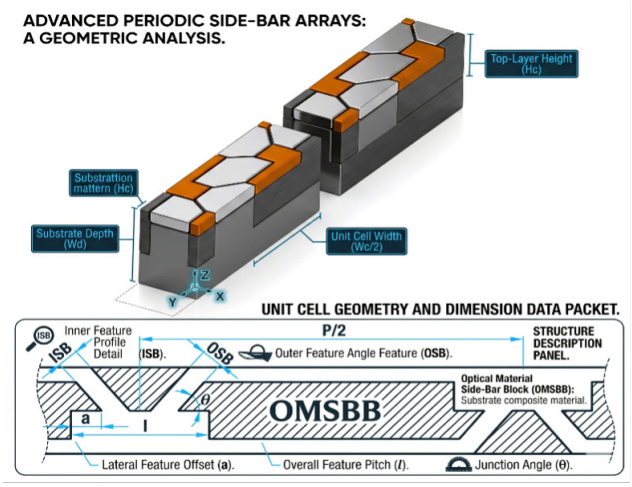


**Figure 20.** Illustration of half of two adjacent MCHS with microchamber, secondary branch, and blockage

### 4.1. Secondary channels and oblique fins

The secondary flow channel is a distinctive intensification of transport phenomena in one of the traditionally efficient heat-transfer techniques. However, the fundamental principle involved is that small-diameter flow passages can readily increase the heat transfer coefficient, supported by vortex flows and boundary-layer reattachment. Kandlikar et al. [33] provided a broad review of remarkable designs of various secondary channel arrangements used in previous studies, transport phenomena application in MCHS, focusing on future research needs based on application and fabrication techniques for low-cost production, as depicted in Figure 15. Previous literature has reported that secondary flows that develop in secondary channels result in an eighty percent enhancement in heat transfer with little pressure drop penalty.

Lee et al. [34] numerically studied the novel design of oblique fin arrangement by breaking continuous fins into oblique sections, as illustrated in Figure 16. They observed that the leading edge of each oblique fin reduced boundary-layer thickness, reinitiated boundary-layer development, sustained the developing flow, and an average increase of 80% in the local heat transfer coefficient. In addition, the arrangement of oblique fins creates a structured flow with secondary flows and entrance effects that lead to a change in temperature gradient of 276.6 K, compared with the conventional channel's 284.8 K. Ghani et al. [35] numerically studied the hybrid technique of ribs with secondary channels for 100 < Re < 500. They compared MC rectangular ribs with MC secondary oblique channels (SOC), the larger flow area in the secondary channel reduced pressure drops by 50%. They achieved the best overall performance of 1.98 at Re = 500. Figure 18. depicts the arrangement of secondary oblique channels with rectangular ribs.

Japar et al. [36] comprehensively studied the novel triangular cavity rectangular rib with a secondary channel (TC -RR-SC) for 100 < Re < 450. They observed the superiority of the design in that its secondary channels caused increased flow mixing and maintained lower static pressure inside cavities than TC-RR, as presented in Figure 17. The performance was exceptional because the temperature consistently decreased due to greater heat removal. The author extended the design to study the influence of secondary channels on hybrid MCHS and sinusoidal cavities, and observed a reduction in pumping power. Shi et al. [37] conducted geometric parameters optimization of secondary channels based on width, angle, and pitch, as shown in Figure 22. With an increase in secondary channel width, pumping power decreases, and thermal resistance increases due to an increase in fluid flow. Thermal resistance and pumping power for an optimized MCHS shows decreases of 28.7% and 22.9%, respectively, compared to a smooth MCHS. The latest techniques of heat transfer that draw attention include flow disruption such as employing ribs are revealed heat transfer enhancement by many authors [33-34], found more fluid mixing. However, this increases the pressure drop penalty. On the other hand, the secondary-channel approaches substantially enhance heat transfer with only minor pressure loss. Combining the three approaches of ribs, cavities and a secondary channel intensifies the flow mixing and

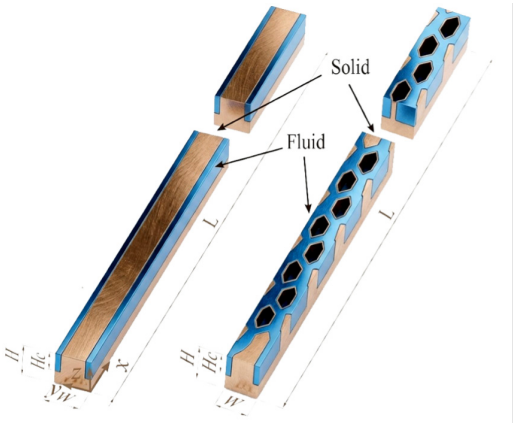


**Figure 21.** Schematic illustration of MCHS designs (a) Smooth MCHS, Fan cavity with secondary channel

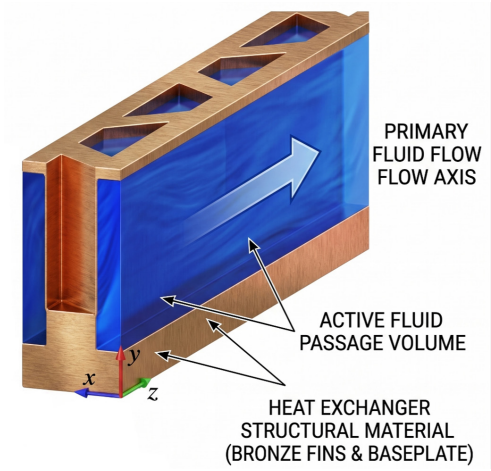


**Figure 22.** Illustration of heat sinks with secondary flow channel computational domain

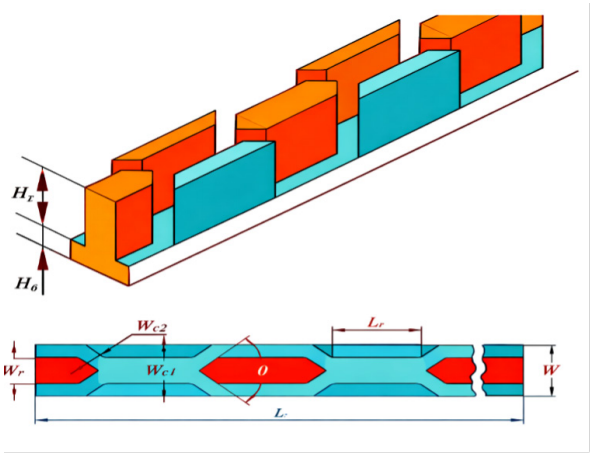

**Figure 23.** SIllustration of staggered diamond ribs (SDR) structure top view and axonometric drawing

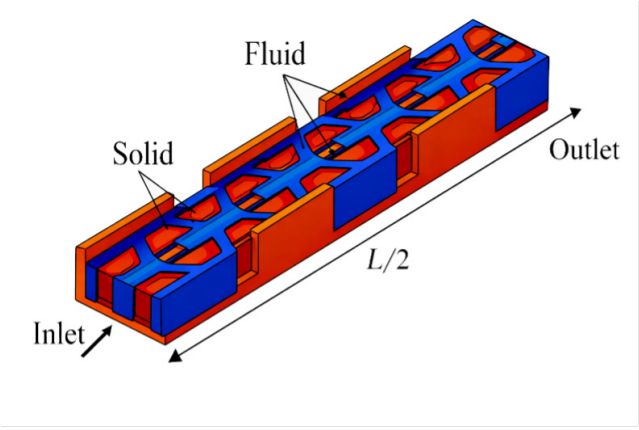


**Figure 24.** Illustration of heat sink equipped with the ribs and secondary channels geometry

makes it more attractive. Bala Subrahmanyam et al. [38-39] conducted three-dimensional conjugate numerical heat transfer analysis with four different ribs placed symmetrically in a fan-shaped cavity (FC) with rectangular rib (RR), backward triangular rib (BTR), forward triangular rib (FTR), and diamond rib (DR). The geometrical parameters are defined as the relative cavity width (α), relative cavity length (β), relative rib width (γ), and relative pitch (λ) to study heat transfer performance. Although a structural optimization study was employed, the results are presented to address existing challenges related to pressure drop. The summary of the analysis is that, of the four proposed rib structures, FC-DR confers an optimal balance between heat transfer and pressure drop and achieves the best thermal performance of 1.97 at Re = 391.47 with silicon as the substrate, as depicted in Figure 21. The author also explored recent innovative designs vapor-filled cavities, ribs, dimples, and protrusions— used to generate flow-disruption effects, and presented the convective heat-transfer performance as a function of Reynolds number. Zhu et al. [40] studied numerically on symmetric wavy MCHS, considered variation in wave crest-to-crest, wave trough-to-trough geometric parameters along slanted secondary channels, as shown in Figure 19. They reported that with an increase in Re from 150 to 300, the vortex formed inside the secondary channel became denser, compared with the central area. The results showed the highest thermal performance of 1.84 at Re=50, the lowest entropy generation number of 0.56 at Re=100 and the most uniform temperature distribution along the length of the channel. Kumar et al. [41] numerically investigated on oblique microchamber with secondary branch and blockage (OMSBB), as depicted in Figure 20. The Nusselt number ratio achieved (1.92) by the configuration without an oblique microchamber dominates up to Re = 397; beyond that, the Nusselt number ratio for the OMSBB configuration continuously increases. Entropy generation due to heat transfer is also much lower, at 0.55. Peng et al. [42] numerically investigated on MCHS with staggered diamond ribs (SDR) as shown in Figure 23, compared with rectangular ribs (RR). The smooth slicing of the diamond rib which acts as a secondary channel and causes mixing of the main flow, clearly shows that the boundary layer's maximum difference in base temperature remains between 289 and 291 K. They also observed a 2.1-fold improvement in the Nu of SDR compared with RR at Re= 500.

### 4.2. Jet impingement, spray cooling and double layered

Several traditional methods for enhancing heat transfer, such as jet impingement, spray-based cooling, and heat pipe-assisted circulation, are widely used because of their efficiency in handling high thermal loads. Another modification researchers proposed is the application of synthetic jets to improve performance. Faghri et al. [43] reviews technological advancement in heat pipes with a number of studies contributed such as loop heat pipes (LHP), micro and miniature heat pipes, pulsating heat pipes (PHP). They observed passive means of heat transport includes lack adaptability in configuration

and often need more physical space to operate effectively in zones of intense heat flux. Additionally, the manufacturing difficulties for micro heat pipes presents significant challenges.

Jambunathan et al. [44] carried out a literature survey on experimental investigations, focused on rate of heat transfer from single circular jet impinging with nozzle orthogonally onto a plane surface. Jet impingement requires considerable pumping power to achieve superior localized heat transfer rates, and precise alignment of nozzles, which together cause high energy consumption to sustain fluid movement. They identified that confinement in the jet causes 4% reduction in heat transfer, and at nozzle-to -plate spacings of less than 10 diameters, the use of an orifice yields a higher rate of heat transfer. Kim et al. [45] reviews spray cooling mechanisms delivers outstanding thermal control, particularly in electronic applications with micro texturing technique, yet faces challenges in sustaining droplet consistency and preventing dry-out conditions. They found a highly efficient thermal management solution, particularly for electronic devices that are exposed to high heat fluxes. However, the complexity of its mechanism and the variability of influencing factors pose challenges in unlocking its full potential.

The combination Mostafa et al. [46] investigated experimentally, numerically on hybrid multilayer MCHS with jet impingement. They reported that a double-layer heat sink produced 7.5% decrease in surface temperature compared with a single-layer heat sink at a reasonable pressure drop. Further, they focused on jet spacings, and the distribution of percentage flow rate between jets and channels, and observed that a smaller number of jets provides better temperature uniformity, while an increase in the number of jets effectively decreases pressure drop. Vamsi et a. [47] experimentally and numerically studied the influence of three inline circular jets impingement effect on heat dissipation. Their experiments were performed at various pitch-to-diameter ratios, dimensionless nozzle-to-plate spacings, and Reynolds numbers. Their results show that as the distance between the target plate and nozzle increases, entrainment losses increase, causing a decrease in the jet velocity impinging on the plate. However, the distribution of the jet over large surface area causes a significant decrease in surface temperature. Chandratilleke et al. [48] studied numerically studied on performance analysis of synthetic Jet mechanism-based hybrid MCHS. The oscillating diaphragm with in a cavity generates a jet that forces the fluid through an orifice. The technique utilizes a strong periodic unsteady jet mechanism called a synthetic jet, which produces very high fluid momentum at a higher diaphragm amplitude of 100 μm and causes intense heat transfer augmentation along the flow passage. They observed heat removal rates 4.3 times higher than those of a smooth channel without the jet mechanism arrangement.

Hoang et al. [49] studied numerically on hybrid multi-jet heat sink, compared rectangular fins with pin-fins, considered different inlet fluid temperatures of $29^0$ C, $36^0$ C, $50^0$ C and $60^0$ C. The higher flow rate increases acceleration and pressure drop, which reduces the effectiveness of cooling. They observed with pin-fin heat sink the chip temperature observed is $2.8^0$ C maximum, also observed lower temperature gradients with cap design of multiple jets arrangement which makes an angle of 9 degree with horizontal plane.

Song et al. [50] investigated numerically on complex design of double-layer structure, compared double layer counter flow and single layer counter flow arrangements. They observed that a double-sided heat sink with complex channels offers lower thermal resistance than a double-sided heat sink with the same structure. Yaghoobi et al. [51] investigated numerically on one to three layers MCHS with different wavelengths and amplitudes at Re from 300 to 1050. Their results indicated that the higher mixing is obtained with a decrease in wavelength, and an increase in channel amplitude, which results in an increased Nusselt number. In channels with increasing amplitude, increased mixing and increased contact surface area between the channel and the fluid are the main causes of the increase in the Nusselt number. Their results showed that the maximum overall efficiencies obtained for one-, two-, and three-layer wavy channels were 1.16, 1.43, and 1.43 respectively.

Ramesh et al. [52] assessed the potential of MCHS research with available data from research articles published from 1996 to 2019. The trend of gradual growth is observed in MCHS research throughout the years. The growth of computer applications reports a massive demand for minimal power consumption and higher thermal performance attracting traditional researchers' focus on more design advancement. Throughout their study, they observed that the pressure drop was the major drawback of MCHS flows. Ghule et al. [53] investigated experimentally and numerically on cross-cut wavy MCHS with cross-cut angles of 0°, 10°, 20°, 30°, 40°and 50°. They considered were nanofluids consisting of a base fluid with colloidal suspensions of particles of 100 nm, with Re in the range of 100-1000. They focused on mechanisms of boundary-layer thinning, boundary-layer rebuilding, and secondary flows. The cross-cut angle of 300 shown significant improvement of 41% in heat transfer, achieved maximum Nusselt number of 11.49.

### 4.3. Nanofluids and nanoparticles

Recent experimental and numerical studies of hybrid nanofluids mixed with water report superior thermophysical properties, such as thermal conductivity, density, specific heat, and viscosity, across different concentrations and temperatures, and demonstrate good stability over time. When nanoparticles are present at low particle volume fractions and small particle sizes, hybrid nanofluids maintain good dispersion stability without producing noticeable penalties in pressure drop. Their analysis revealed fluid dynamic behaviour, which provides valuable insights for the design optimization of conventional cooling mechanisms, including: (i) contin-

uous interruption in the development of the boundary layer and increased turbulence; (ii) increased heat transfer area; and (iii) generation of secondary flows.

Despite their promising properties, the nanofluids face challenges such as low stability in aqueous solutions, an increase in viscosity leading to increased pumping power, channel erosion, corrosion, clogging, fouling, and high production cost, thereby limiting their applicability in the cost-effective production of nanofluids. However, hybrid nanofluid, due to its dynamic thermal modes that exceed steady-state dissipation, influences the tunability of flow-structure mechanisms inside microchannels and promotes local heat transfer coefficients along the channel length. Furthermore, especially hybrid nanofluids variants that includes a nanoparticles combination of alumina oxide (Al2O3), copper (Cu), silver (Ag), iron oxide (Fe3 O4) with metallic-oxide and carbon additive studies exploration leads to a substantial enhancement in thermal performance [74-76]. Significant challenges in the application of nanofluids, such as ensuring stability, at varied proportions of the nanoparticle blend which can potentially limit their effectiveness, need further exploration.

Liu et al. [54] investigated numerically on five different arrangements of column rib with multiple jet impingement (MJI) with nanofluid concentration (1% to 5%). The column ribs arranged behind the jet holes cause deepening of longitudinal vortex flow that causes formation of additional vortices, an improvement of heat transfer coefficient h. They have observed the highest thermal performance of 1.75 at nanofluid concentration of 1% and at Re=400. Kuppusamy et al. [55] numerically examined trapezoidal grooved MCHS heat sinks (TGMCHS), focused on a groove geometry-based parametric study. They considered groove widths, pitch, and groove angle, as presented in Figure 14. Changing the groove shape from rectangular to triangular substantially improved thermal performance. The increment achieved in thermal performance is 91.43%, and that in the Nusselt number is 120.2%. The liquid flow through the wavy channel generates secondary flows (Dean vortices) that induce chaotic advection, depending on the vortices' locations. The improved fluid mixing enhances heat transfer performance much more than rectangular channels do.

Bahiraei et al. [56] numerically investigated by incorporating combination of ribs, secondary channels, as presented in Figure 24 and hybrid nanofluids containing graphene–silver nanoparticles. They observed the lowest bottom-wall temperature of 13.88 K as Re increased from 100 to 500, and an improvement in the convective heat transfer coefficient of 17% at Re of 100. The increment is much more effective when the nanofluid concentration is 0.1%. Sarafraz et al. [57] investigated experimentally on gallium liquid metal enriched with aluminium-oxide nanoparticles in a MCHS solar thermal receiver. They focused on designing next-generation solar thermal energy receivers equipped with MCHS fluid passages. At a mass fraction of 10%, increasing thermal conductivity rises the thermal performance index to 3.5 and 2.9 in the laminar and turbulent regimes, respectively

**Table 2.** Summary of important investigations based on hybrid cooling approach of Nanofluids flow for comparative study in MCHS based on TP

| Authors | Experimental/Numerical, Hybrid Nanofluids/Nanotubes composition | Enhancement in Nu/Heat transfer coefficient (or) Detraction in thermal resistance | Pressure drop penalty/ Friction factor |
|---|---|---|---|
| Chu et al. [70] | Numerically, alumina nitride (AIN)-alumina oxide (Al2O3)–water | Enhancement in heat transfer coefficient from 21.13% to 43.77%. | 24.13 Pa to 205.13 Pa Pressure drop penalty increased |
| Qu et al. [71] | Numerically, magnetic iron oxide (Fe3O) /graphene nanofluid. | Detraction in thermal resistance from 1.5% to 1.1%. | 16.1% to 31.4% Pressure drop penalty increased |
| Nabi et al. [72] | Numerically, single-walled carbon nanotubes (SWCNTs) and multi-walled carbon nanotubes (MWCNTs). | Enhancement in heat transfer coefficient from 19.1% to 56.1%. | 9.3% to 48.8% Pressure drop penalty increased |
| Rajesh et al. [73] | Numerically, suspension of both alumina ($Al_2O_3$) and silver (Ag) nanoparticles in water. | Enhancement in heat transfer coefficient from 128% to 146%. | ---------- |

| | | | |
|---|---|---|---|
| Takabi et al. [74] | Numerically, aluminum oxide (Al2O3) and copper (Cu) nanoparticles in water. | Enhancement in Nu of 32.07% | the friction factor expense of 13.76% |
| Suresh et al. [75] | Experimentally, water-based fluids with suspended nanoparticles of both aluminum oxide ($Al_2O_3$) and copper (Cu). | Enhancement in Nu of 16.97% | Pressure drop penalty of 16.97% increased |
| Sundar et al. [76] | Experimentally, water with both multi-walled carbon nanotubes (MWCNTs) and iron (III) oxide (Fe3 O4). | Enhancement in Nu of 31.1% | Pressure drop penalty of 1.86% increased |
| Yarmand et al. [77] | Experimentally, both graphene nanoplatelets (GNP) and silver nanoparticles. | Enhancement in Nu of 32.7% | the friction factor expense of 1.08 times |
| Megatif et al. [78] | Experimentally, water-based liquid with suspended titanium dioxide (TiO2) nanoparticles-carbon nanotube (CNT) | Enhancement in Convective heat transfer coefficient of 38% | from 0.96 Centipoise to 0.99 Centipoise (Dynamic viscosity increased) |
| Madhesh et al. [79] | Experimentally, copper-titanium nanocomposite (HyNC) dispersed in the water | Enhancement in Nu of 49% | 14.9% Pressure drop penalty increased |

Souby et al. [58-59] numerically investigated on hybrid nanofluid (HNF) of reduced graphene oxide decorated with cobalt oxide nano composite and ferrous oxide flow with 0 to 0.2% concentrations range for improvement in hydrothermal performance and second law characteristics. The heat transfer coefficient increases with nanofluid concentration. At a concentration (φ) of 0.2% of multi-walled carbon nanotube-magnetite, the heat transfer coefficient (h) increased by 22.1% at Re of 300 and by a further 13.3% at Re of 1500; an improvement in thermal conductivity was also observed The author extends the numerical investigation to rectangular-shaped ribs and the design of secondary flow passages, with nanofluid concentration (Φ) ranging from 0 to 0.5 % and Re from 100 to 500. They investigated the flow of graphene quantum dots (GQDs) nanofluid to minimize sedimentation effects and entropy generation, and to maximize hydrothermal performance. The improved thermal conductivity has been played a significant role in achieving improvement in convective heat transfer coefficient of 24.9% and decrement in total entropy generation of 14.7% at Φ of 0.5, at lower Re of 100.

Najafpour et al. [60] studied numerically on angled fin heat sink (AFHS), positioned at different angles of 0°, 30°, 60°, and 90° relative to the flow direction by the use of a ternary hybrid nanofluid that consists of zinc and aluminium oxide nanoparticles at different volume fractions in the range of Re from 800 to 1600. They considered three different volume fractions of nanoparticles (2 %, 4 %, and 6 %) flowing over the fins at Re of 1200 and observed pressure drops of 200 Pa, 500 Pa, and 800 Pa, respectively. At a fin angle of 60° relative to the flow direction, a Nusselt number improvement of 33.20 % was observed, along with temperature uniformity. Arshad et al. [61-62] studied numerically on novel combination of metallic oxides (silver, magnesium), carbon-based nanofluids (graphene nanoplatelet, multi-walled carbon nanotube) flow over aluminium made circular pin-fin by adopting the multiphase Eulerian model in first part, circular and rectangular pin-fin configurations considered in second part at constant volume fraction to improve cooling efficiency. The advanced graphene-nanoplatelet-dispersed monofluids indicate substantial heat dissipation capability and improved stability, resulting in a 46.41% reduction in thermal resistance and a 60.54% increase in average Nu value compared to conventional water cooling. Consequently, the highest performance was also achieved at a 60% volume fraction of graphene nanoplatelets. Veeraraghavan et al. [63] conducted a comparative study of synthesized composite nanofluids (CNF) and conventional hybrid nanofluids (HNF) for rectangular MCHS in experimentally and numerically. The comparative study reveals that at Re of 900 heat transfer co-efficient (HTC) achieved of 2055 $W/m^2.K$, correspondingly 24 % improvement for CNF due its superior stability and morphology properties, compared to pure water case and HNF has been achieved lower HTC of 1890 $W/m^2.K$, resulting in an enhancement of around14 %. However, achieves 40% higher thermal performance than CNF.

Chen et al. [64] studied numerically and experimentally on manifold MCHS with copper nanoparticles flow with volume fraction variation from 0 to 6%, focused on topology optimization to improve thermal performance. The copper nanoparticles have been shown to have high thermal conductivity and to significantly improve heat transfer. They observed that at lower Re values, a greater number of branches exhibited the best performance. However, the particle volume fraction reduces the influence of particle diameter. They concluded that at 100 nm particle diameter, 0.5% particle volume fraction of nanofluid under optimal topology design produced heat transfer performance of 11.4% higher than conventional parallel flow channel.

Kamsuwan et al. [65] studied numerically on Polymer-based MCHS, considered three dissimilar nanofluids of aluminium, titanium and copper oxides along water as base fluid, constructed artificial neural network (ANN) model in order to predict nanofluid properties including viscosity, density, thermal conductivity and heat capacity using MATLAB. The results showed that titanium oxide with water as the base fluid, exhibited a 12% increase in overall heat transfer coefficient compared with water, and the highest performance index across all Re values tested. Liao et al. [66] investigated numerically on aluminium oxide nanofluid flow over vortex generators with testing parameters ranges for blockage ratios in the range from 0.05 to 0.8, aspect ratios from 0.5 to 20 and nanoparticle volume fraction from 0 to 6%. They identified that an aspect ratio of 0.5 exhibits a strong, widespread localized vortex, as the aspect ratio increases, the resulting flow stability causes a local reduction in the intensity of heat transfer near the vortex generator. However, reduced yield balanced heat-transfer gains while incurring minimal mechanical penalties. They concluded that, at a nanofluid volume fraction of 6 %, the mean Nu improves by 15.7 % compared with base fluid for a pressure drop increase of 3.4 %. Suja et al. [67] conducted a numerical study on different nanofluids of copper, aluminium and titanium dioxide dispersed in water–ethylene glycol mixtures at two volume fractions of 0.5 % and 2 % flow over three different configurations of inline, staggered, and $45^0$ inline, extensively focused various porosity values from 40 to 60% on the thermal and fluidic behaviour. The numerical results showed that 2.8 % lower temperature with water-based copper oxide and $45^0$ inline configuration exhibited temperature that was 0.852 % lower than inline and 0.63 % lower than staggered arrangements. Tuaima et al. [68] investigated experimentally and numerically compared straight, zigzag, wavy, and circular cavities heat sinks with copper oxide nanofluid flow with volumetric concentration of 0.01, 0.02, and 0.03 and Re ranges from 50 to 150. At Re of 150, and a heat flux of 170 kW/m², they observed 12% increase in Nu values with the wavy channel and the mean wall temperature of 34.2°C at volume concentration of 0.03%. In contrast, under the same conditions, the highest mean wall temperature 53.2°C, was observed. Goksu et. [69] investigated numerically on oxides of copper and ferrous mono-hybrid nanofluid at 1% concentration of each flow over eight different block configurations which includes horizontal and vertical geometries. They focused on parameters including spacing, block thickness, and flow direction for minimizing thermal resistance and maximizing based on performance evaluation criteria (PEC) was achieved 0.28 K/W and 1.04 respectively. Chu et al. [70] numerically investigated the heat transfer and fluid flow characteristics in a straight MCHS having a circular cross section. Their investigation was carried out over the Reynolds number (Re) range of 15-65, using water containing a hybrid nanofluid (alumina nitride (AIN) and alumina oxide ($Al_2o_3$) at volume fractions of 1%, 2%, 3%, and 4%. They observed that a higher Nusselt number (Nu) was obtained with the hybrid nanofluid than with water alone. They also noticed decrease in the friction factor and thermal resistance, and an increase in Nu as Re and the volume fraction of the hybrid nanofluid increased. They concluded that water with hybrid nanofluid enhanced the heat transfer coefficient by 21.13% to 43.77% while the pressure-drop penalty increased from 24.13 Pa to 205.13 Pa for Re in the range 15 to 65, compared with water alone.

Qu et al. [71] analytically investigated the hydrothermal characteristics in straight MCHS using the multi-objective particle swarm optimization (MOPSO) technique. In their analysis, the working fluid was water, with the hybrid Nanofluid ($Fe_3O_4$/graphene) used at mass fractions of 0.1, 0.3, and 0.5 wt%. They identified and developed the optimized MCHS that is suitable for higher heat dissipation. They observed that thermal resistance decreased as nanofluid concentration increased. They concluded that water containing pure graphene nanofluid exhibited a decrease in thermal resistance, with a pressure-drop penalty of 16.1% to 31.4% at mass fractions of 0.1, 0.3, and 0.5 wt%, respectively.

Nabi et al. [72] numerically investigated the heat transfer and fluid flow characteristics in various models such as Simple, Ternate veiny, Honeycomb, Snowflake, and Spider netted. Their investigation has been carried out in the Re ranges from 200 to 800 at various heat flux applied in between 35 to 350 KW/$m^2$ and treated the working fluid as water with Nanofluids (Multi-Walled Carbon Nanotubes (MWCNTs) and Single-Walled Carbon Nanotubes (SWCNTs)) at various volume fractions of 1%, 2% and 3%. They concluded that water containing SWCNTs exhibited better performance than water containing MWCNTs. They also noted that the spider-net model exhibited a higher heat transfer coefficient, ranging from 19.1% to 56.1% with a pressure drop penalty of 9.3% to 48.8 compared with other models at Re 500. Rajesh et al. [73] numerically investigated the heat transfer characteristics of hybrid Nanofluid with water in a straight MCHS having a rectangular cross-section. In their studies, they treated the working fluid as a hybrid nanofluid, i.e., water containing aluminum oxide ($Al_2O_3$) and silver (Ag). They observed that the heat transfer coefficient has increased from 128% to 146% for 0.6 vol.% $Al_2O_3$ + 2.4 vol.% Ag in water, compared with water alone. Takabi et al. [74] numerically investigated the heat transfer and fluid flow characteristics of water with hybrid Nanofluid (Al2O3–Cu) in a circular tube. They observed that Nu increased by 32.07% at a 0.1% volume fraction of the given hybrid Nanofluid, at the expense of a 13.76% increase in the friction factor.

Suresh et al. [75] experimentally investigated the thermo-physical properties of hybrid Nao fluid (Al2O3–Cu) with water as base fluid in various volume fractions of 0.1%, 0.33%, 0.75%, 1%, and 2%. They concluded that water with a hybrid nanofluid exhibited an enhancement in Nu of 16.56% and a pressure drop penalty of 16.97% at Re 1730 compared with water alone. Sundar et al. [76] experimentally investigated the hydrothermal characteristics of fully developed turbulent fluid flow in a circular tube. In their investigation, they used a hybrid nanofluid (MWCNT–$Fe_3O_4$) at volume fractions of 0.1% and 0.3%, with water as the base fluid. They concluded that a 0.3% hybrid nanofluid with water as the base fluid exhibited an enhancement in Nu of 31.1% with a pressure drop penalty of 1.86% at Re 22,000. Yarmand et al. [77] experimentally investigated the significance of a hybrid Nanofluid (silver and graphene nanoplatelets) with water as the base fluid, on the hydrothermal characteristics of fully developed turbulent fluid flow in a circular tube. They concluded that Nu increased by 32.7% with a 0.1% mass fraction of hybrid nanofluid at Re 17,500, accompanied by a 1.08-fold increase in the friction factor compared to water alone. They also developed an empirical correlation, based on their experimental results, to calculate Nu and the friction factor.

Megatif et al. [78] experimentally investigated the significance of a hybrid Nanofluid (TIO2 –Carbon Nanotube) with water as the base fluid, on the hydrothermal characteristics of laminar fluid flow in a shell-and-tube heat exchanger. They concluded that the convective heat transfer coefficient increased by 38% at a 0.2% mass fraction of the hybrid nanofluid; they also noted that the overall dynamic viscosity increased from 0.96 cp to 0.99 cp as the mass fraction of the hybrid nanofluid increased from 0.1% to 0.2%. Madhesh et al. [79] experimentally investigated the significance of a hybrid Nanofluid (Cu-TiO2) with water as the base fluid, on the hydrothermal characteristics of fluid flow in a tubular heat exchanger. They observed that Nu increased by 49% with a pressure drop of 14.9% at 0.1% volume fraction of hybrid nanofluid (Cu-$TiO_2$).

### 4.4. Pin fins

Pin-fin arrays of different geometrical shapes with small cylinder-size designs and orientations used to increase heat transfer and with potential for high efficiency, provide lower pressure drop. The experimental and numerical studies demonstrated that an increase in surface area for heat transfer is advantageous compared with conventional fins. Jani et al. [80] investigated numerically on rectangular pin-fin with copper, aluminium, titanium, and structural steel substrate materials. As the Reynolds number increases and Young's modulus decreases intense fluid mixing reduces thermal stresses, increased deformation is also observed at the mid-section. The highest Nusselt numbers are observed for highly thermally conductive materials, such as copper and aluminium. Alihosseini et al. [81] studied numerically on Hybrid MCHS, considered case 1 to 5, straight, circular pin-fin, straight-circular pin-fin-straight, oblique grooved straight-circular pin-fin-oblique grooved straight, oblique grooved straight-circular pin-fin-oblique grooved straight reversed. The hybrid design of pin-fins together with grooves promotes the disruption of the boundary layer and the formation of secondary flows, leading to improved heat transfer, which can reduce the risk of hot spots on the chip. The results suggest a novel geometrical design and indicate that at Re of 1250, Nu values for cases IV and V achieved 517.7 % and 525.1 % improvements, respectively, compared with the straight channel (case I). Raafat et al. [82] conducted numerical investigation using hybrid designs combinations of I-graph wrapped package (IWP)-graph along with square pin fin, triply periodic minimal surfaces (TPMS). They mainly focused on topology design, which promotes minimal blockage, and the formation of secondary cooling jets to achieve higher Nu values. Their research produced a 54% reduction in pressure drop, a 27% improvement in thermal efficiency with the IWP package, and a significant balancing of pressure drop and heat transfer.

## 5. Heat sink material and microchannel fluids

Many researchers Xie et al. [83], Xia et al. [84], Kuppusamy et al. [85], Vinodhan et al. [86], Sui et al. [87], Mohammed et al. [88] etc. in their theoretical and experimental works used silicon as channel material while Ghani et al. [35], Deng et al. [89], Lee et al. [90], Yan Fan et al. [91] etc. used silicon and copper as channel material. Copper is often preferred because of its high ductility, good machinability, high strength, ease of joining, good surface quality, corrosion resistance, and excellent thermal conductivity, which enables rapid and uniform heating. The working fluids most commonly used in microchannels are air, water, and refrigerants. Tullius et al. [92] reviewed microchannel cooling studies and summarized the selection of fluids for different applications based on their heat transfer performance and transport properties. Air is not preferable for cooling in miniaturized electronic applications with high heat dissipation, whereas liquids that can handle heat fluxes above 100 W/cm² are preferred in microchannels. Most liquid coolants, such as water, ethylene glycol, and refrigerants, offer higher convective heat transfer coefficients and specific heat capacities, making them effective for high heat dissipation. Incropera et al. [93] provided a detailed qualitative comparison of heat transfer coefficients for different fluids, as shown in Figure 25. In microchannels, heat transfer performance is affected not only by fluid properties but also by factors such as channel geometry, wall surface conditions, and the presence of grooves, cavities, or extended fins on the inner and outer surfaces of the channel.

### 5.1. Microchannel fabrication and cost analysis

Many researchers have attempted to fabricate novel packages, and have observed certain challenges in the preparation of heat exchangers; addressing technological challenges is necessary to enable structural optimization and to overcome limitations in cost-effectiveness. Furthermore, the study explored the advantages of additive manufacturing owing to its more effective bonding capability between substrate materials compared with conventional manufacturing techniques such as sintering, chemical etching, micromachining,

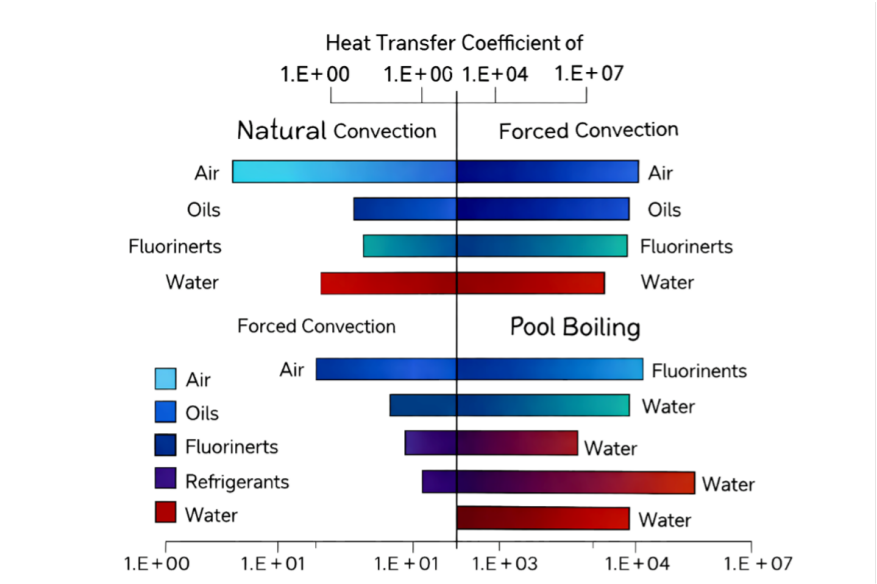


**Figure 25.** Thermal properties of different fluids of convection flow

micro-discharge, and laser processing. Gao et al. [94] in their study, presented the various methodologies and manufacturing technologies of microchannel fabrication for economic and environmental impacts. They introduced a methodology that provided the practical framework for evaluating the economic and environmental aspects of microchannel manufacturing. Gao et al. [95] introduced the framework model to assess the microchannel material cost, fabrication cost, production sales, energy consumption, and environmental impacts. They noticed that the framework model serves as an effective tool for estimating and optimizing microchannel manufacturing costs. Nicholas et al. [97] studied the various manufacture techniques used to produce rounded microchannels in polydimethylsiloxane (PDMS). These techniques were evaluated based on channel geometry, surface roughness, durability, manufacturing difficulty, and cost estimates. A comparative investigation of fabrication methods for generating rounded microchannels in PDMS reveals that the technique employed considerably affects channel geometry, surface quality, and device performance. Thermal reflow, grayscale lithography, and isotropic etching techniques improve control over rounded channel profiles and produce smoother surfaces, which are advantageous for minimizing pressure drop and improving laminar flow behaviour. However, these processes frequently necessitate precise process control, specialized equipment, and increased fabrication costs. They concluded that there is no single best fabrication technique. Rather, application-specific considerations such as the desired channel geometry, flow performance, repeatability, production volume, and cost limits should direct the choice. Awareness of the trade-offs associated with each technique enables educated decisions and promotes the optimal design and production of PDMS-based microfluidic devices with rounded microchannels. Wilson et al. [98] studied the design and development of a high-temperature, low-cost silicon carbide microchannel. They noticed that silicon carbide is a suitable material for microchannel fabrication. It is attributable to its higher thermal conductivity, corrosion and thermal-shock resistance, and greater strength at elevated temperatures. They suggested various manufacturing techniques for microchannel fabrication, including extrusion, tape casting, additive manufacturing, and joining and sealing methods. They observed that extrusion and tape casting reduced manufacturing costs compared with other manufacturing techniques. They suggested that silicon carbide microchannels have good compatibility with various working fluids, such as air, nitrogen, combustion exhaust gases, helium, and supercritical carbon dioxide. They also suggested silicon carbide microchannels for the thermal management of micro gas turbines, solid oxide fuel cells, industrial waste heat recovery devices, and aerospace applications. Gregory et al. [99] studied the design and manufacture of integrated microchannels and inlet and outlet manifold on a discrete silicon (low-cost polycrystalline silicon) channel substrate. These improve fluid distribution, structural strength, and thermal performance in microchannel devices while reducing manufacturing costs. Separating the microchannel and manifold simplifies fabrication, and provides greater design flexibility. Low-cost polycrystalline silicon offers performance comparable to single-crystal silicon, making the approach well-suited for high-density microfluidic and thermal management applications. Collins et al. [100] investigated experimentally on additively manufactured (AM), compared with direct metal laser sintered (DMLS) MCHS and established correlations in order to identify challenges associated with AM technique. They observed that an AM-based channel induced an early transition from laminar to turbulent flow at Re below 800 for both straight and manifold heat sinks, which restricts the applicability of standard laminar-flow correlations. However, the predicted laminar-flow Nu was 45% higher than the measured value for the straight channel, and the AM-based com-

plex-geometry manifold channel exhibited a 40 to 90% reduction in pressure drop compared with the straight-channel design over a flow range of 100 mL/min to 500 mL/min.

## 6. Conclusion

In the present paper, an effort has been made to summarize experimental and numerical investigations of active heat-transfer-enhancement techniques for liquid flow in MCHS, focusing on heat transfer and pressure-drop characteristics. The content is divided into: first, the basic concept of smooth/rectangular channels and second, flow disruptions, which include extended surfaces (fins/ribs), interruptions, bifurcations, cavities/grooves, secondary channels/oblique fins, and advanced cooling methods such as hybrid nanofluids/multi-walled nanotubes, jet impingement, and pin fins. The nanofluid with varying particle concentrations exhibits improved thermal conductivity and performance. It aims to conduct a comparative study of methods for maximizing the convective heat transfer coefficient by addressing reported by previous researchers. Different design approaches, can minimize the laminar stagnation zone; for example. restricting fluid slip over re-entrant cavities can be achieved with ribs that enhance flow disturbance and regulate the maximum temperature near the substrate bottom wall at the outlet region; substrate material selection, operating conditions, and working fluid thermophysical properties also influence this.

However, many studies have examined how different channel geometries, such as, circular, rectangular, triangular, trapezoidal, wavy shape designs can augment heat transfer increment based on the area available. The study also focused on various types of nanofluids such as alumina oxide, magnetic iron oxide ($Fe_3O$) /graphene, silver (Ag) nanoparticles, copper (Cu), titanium dioxide ($TiO_2$) nanofluid along with water. The redevelopment of the thermal boundary layer results in more significant heat transfer coefficients was proven by many authors, profound enhancement is observed based on entrance effect. Further advancement is observed through their experiments based on thermal design corresponding to shape, geometrical parameters of cavities, ribs, and secondary channels combination. The extensive design strategies come across in previous literature study on MCHS, some recommendations based on the current review work are

- It was identified that geometric parameters, such as cavity width, cavity length, rib width, rib length, and aspect ratio associated with channel-shape optimization, make it possible to control an appropriate balance between coolant temperature and wall temperature. In terms of application, new substrate materials and coolants, such as hybrid nano/monofluids with improved thermo-physical properties, show cooling potential through heat transfer enhancement.
- As heat sink geometry like rib arrangement inside cavities, to the side walls and also with addition of connecting secondary channels plays key role in heat transfer enhancement, most numerical studies observed are based on vortex growth, change of flow structure, topology optimization, stirring of the hot and cold streams, still many more innovative designs need to be tested.
- Application of an advanced ternary hybrid nanofluid consisting of zinc and aluminium oxide nanoparticles to fins provided a Nusselt number improvement of 33.20 %. The base fluids most commonly used are water and ethylene glycol (EG) hybrid nanoparticle combinations, including oxides of Zinc (ZnO), Copper (CuO), Aluminum ($Al_2O_3$), Titanium ($Tio_2$) exhibit a 40% higher thermal performance.
- Geometric advancements in hybrid designs (fin/rib structures and secondary channels), parameter optimization based on multi-physics analyses, and hybrid nanofluids at different concentrations have been found to enhance heat transfer while minimizing pressure drop. These findings have significant implications for the industry and warrant further investigation. The pin fins with advanced nanoparticles of silver and magnesium and carbon-based nanofluids such as graphene nanoplatelets and multi-walled carbon nanotubes showed a Nu improvement of 60.54%.
- The design of the header is crucial for achieving optimal heat transfer enhancement. The arrangement, shape, and position of the inlet and outlet, and the selection of headers, can adversely affect pressure drop, particularly as flow rate increases. The Z-type manifold design has been achieved the ultra-high heat dissipation to date. Therefore, it is advisable to explore the design of manifolds further.

## Acknowledgements

This research was conducted at Sri Vasavi Engineering College, Pedatadepalli, Tadepalligudem, and at NIT Agartala, Agartala, and did not receive any specific grant from funding agencies in the public, commercial, or not-for-profit sectors.

## Disclosure of interest

No potential competing interests were reported by the authors.

## Nomenclature

| | |
|---|---|
| $A_{con}$ | Convective heat transfer area ($m^2$) |
| B | Pitch distance (m) |
| $C_p$ | Specific heat capacity ($Jkg^{-1}K^{-1}$) |
| Dh | Hydraulic diameter (m) |
| f | Friction factor |
| kPa | Kilo pascal |
| h | Heat transfer coefficient (Wm−2 K−1) |
| H | Height of the channel (m) |
| k | Thermal conductivity ($W.m^{-1}K^{-1}$) |
| L | Length of the channel (m) |

| | |
|---|---|
| Nu | Average Nusselt number |
| p | Pressure (Pa) |
| $q_w$ | Heat flux at bottom of sink ($W.m^{-2}$) |
| Re | Reynolds number |
| T | Temperature (K) |
| $u_{in}$ | Inlet velocity of fluid ($m.s^{-1}$) |
| x,y,z | Cartesian coordinates (m) |
| X,Y,Z | Dimensionless coordinates |
| w | Width of the channel (m) |
| *D* | Pitch of the channel (m) |
| $N_{S,a}$ | Entropy generation number |
| Φ | Nanofluids concentration |

## Subscripts

| | |
|---|---|
| c | Cavity |
| 0 | Smooth rectangular microchannel |
| r/R | Rib |
| s | Solid |
| B | Base |

## Abbreviations

| | |
|---|---|
| MCHS | Microchannel heat sink/sinks |
| PEC | Performance evaluation criteria |
| TP | Thermal performance |
| NSGA | Non-dominated sorting genetic algorithm |
| CPV | Concentrator photovoltaic |
| CR | Concentration ratios |
| DL | Double layered |
| MC | Microchannel |
| SOC | Secondary oblique channels |
| PV | Photovoltaics |
| VLSI | Very large-scale integration |
| MJI | Multiple jet impingement (MJI) |
| SM | Smooth microchannel |
| OSB | Oblique with secondary branch |
| μm | Micrometres |

## Copyright and permission statement

All the illustration Figures of different microchannel designs were drawn using license copy of Google Gemini platform of Universiti Malaysia Pahang Al-Sultan Abdullah, Pekan, Malaysia.

## References


[1] D.B. Tuckerman, R.F.W. Pease., (1981)., High-performance heat sinking for VLSI, IEEE Electron, Device Lett. 2 126–129. https://doi.org/10.1109/EDL.1981.25367.

[2] Webb, R.L. (1981)., "Performance evaluation criteria for use of enhanced heat transfer surfaces in heat exchanger design", International Journal of Heat and Mass Transfer, v. 24, n. 4, pp.715-726. https://doi.org/10.1016/0017-9310(81)90015-6.

[3] Steinke, M. E., and Kandlikar, S. G., (2004)., "Single-Phase Heat Transfer Enhancement Techniques in Microchannel and Minichannel Flows", ASME 2nd International Conference on Microchannels and Minichannels, June 17–19, Rochester, NY. https://doi. org/10.1115/ICMM2004-2328.

[4] Kroeker, C.J., Soliman, H.M. and Ormiston, S.J., (2004)., "Three-dimensional thermal analysis of heat sinks with circular cooling micro-channels", International Journal of Heat and Mass Transfer, v. 47(22), pp.4733-4744. https://doi. org/10.1016/j.ijheatmasstransfer. 2004.05.028.

[5] Prasher. R., (2006)., "Thermal Interface Materials: Historical Perspective, Status, and Future Directions", Proceedings of the IEEE, v. 94, n. 8, pp. 1571-1586. https://doi.org/ 10.1109/ JPROC.2006.879796.

[6] Mahalingam, M., (1985)., "Thermal management in semiconductor device packaging", Proceedings of the IEEE, v. 73(9), pp.1396-1404. https://doi.org/10.1109/PROC.1985. 13300.

[7] Kishimoto, T. and Saski, S., (1987)., "Cooling characteristics of diamond-shaped interrupted cooling fin for high-power LSI devices", Electronics Letters, v. 9(23), pp.456-457. https:// doi.org/10.1049/el:19870328.

[8] Phillips, R. J., (1987)., "Forced-Convection, Liquid-Cooled Micro Channel Heat Sinks",M.S. Thesis, Massachusetts Institute of Technology, Cambridge, MA.

[9] Harpole, G.M. and Eninger, J.E., (1991)., "Micro-channel heat exchanger optimization", Proceeding of the 7th IEEE SEMI-THERM Symposium (pp. 59-63). https://doi.org/ 10.1109/ STHERM.1991.152913·

[10] Sharma, C.S., Tiwari, M.K., Zimmermann, S., Brunschwiler, T., Schlottig, G., Michel, B. and Poulikakos, D., (2015)., "Energy efficient hotspot-targeted embedded liquid cooling of electronics", Applied Energy, v.138, pp.414-422. https://doi. org/10.1016/j.apenergy. 2014.10.068.

[11] Yang, S., Li, J., Cao, B., Wu, Z. and Sheng, K., (2024)., "Investigation of Z-type manifold microchannel cooling for ultra-high heat flux dissipation in power electronic devices", International Journal of Heat and Mass Transfer, v.218, pp.124792. https://doi.org/10.1016 /j.ijheatmasstransfer.2023.124792.

[12] Kuppusamy, N.R., Mohammed, H.A. and Lim, C.W., (2014)., "Thermal and hydraulic characteristics of nanofluid in a triangular grooved microchannel heat sink (TGMCHS)", Applied Mathematics and Computation, v.246, pp.168-183. https://doi.org/ 10.1016/j.amc.2014.07.087.

[13] Wu, P. and Little, W. A., (1983)., "Measurement of friction factors for the flow of gases in very fine channels used for microminiature refrigerators", Cryogenics, v. 24, pp. 273-277. https://doi.org/10.1016/0011-2275(83)90150-9.

[14] Wu, P. and Little, W.A., (1984)., "Measurement of the heat transfer characteristics of gas flow in fine channel heat exchangers used for microminiature refrigerators", Cryogenics,v. 24(8), pp.415-420. https://doi.org/10.1016/0011-2275(84)90015-8.

[15] Peng, X.F., Peterson, G.P. and Wang, B.X., (1994)., "Heat transfer characteristics of water flowing through microchannels", Experimental Heat Transfer an International Journal, v. 7(4), pp.265-283. https://doi.org/10.1080/08916159408946485.

[16] Peng, X.F., Peterson, G.P. and Wang, B.X., (1994)., "Frictional flow characteristics of water flowing through rectangular microchannels", Experimental Heat Transfer an International Journal, v. 7(4), pp.249-264. https://doi.org/10.1080/08916159408946484.

[17] Xia, G.D., Jiang, J., Wang, J., Zhai, Y.L., Ma, D.D., (2015)., "Effects of different geometric structures on fluid flow and heat transfer performance in microchannel heat sinks", International Journal of Heat and Mass Transfer, v. 80, pp. 439–447. https://doi.org/ 10.1016/j.ijheatmasstransfer.2014.08.095.

[18] Savino, S. and Nonino, C., (2024)., "Thermal Performance Improvement of Cross-Flow Double-Layered Microchannel Heat Sinks through Proper Header Design", Energies, v. 17(15), p.3790. https://doi.org/10.3390/en17153790. [Permission and distribution of Material is License from MDPI, Basel, Switzerland under the terms and conditions of the Creative Commons Attribution (CC BY) license]

[19] Shao, H., Wang, Z., Liao, M., Li, C., Liang, Z. and Zhao, Q., (2023)., "Shape optimization of inlet header of micro-channel heat sink using surrogate model combined with genetic algorithm", Thermal Science, v. 27(6 Part A), pp.4551-4564. [Permission and distribution of Material is License from Vinča Institute of Nuclear Sciences, Belgrade, Serbia under the terms and conditions of the Creative Commons Attribution license (CC BY-NC-ND 4.0)]

[20] Lorenz, E.N., (1963)., "Deterministic non-periodic flow", Journal of atmospheric sciences, v. 20(2), pp.130-141. https://doi.org/10.1175/1520-0469.

[21] Gunnasegaran, P., Mohammed H.A., Shuaib, N.H., Saidur, R., (2010)., "The effect of geometrical parameters on heat transfer characteristics of microchannels heat sink with different shapes", International Communications in Heat and Mass Transfer, v. 37, pp. 1078–1086. https://doi.org/10.1016/j.icheatmasstransfer.2010.06.014.

[22] Wang, H., Chen, Z., Gao, J., (2016)., "Influence of Geometric Parameters on Flow and Heat Transfer Performance of Micro-Channel Heat Sinks", Applied Thermal Engineering, v.107, pp. 870-879. https://doi.org/10.1016/j.applthermaleng.2016.07.039.

[23] Jubran, B.A. and AI-Salaymeh, A.S., (1996)., "Heat transfer enhancement in electronic modules using ribs and "film-cooling-like" techniques", International journal of heat and fluid flow, v.17(2), pp.148-154. https://doi.org/10.1016/0142-727X(95)00098-B.

[24] Chai, L., Xia, G.D. and Wang, H.S., (2016)., "Numerical study of laminar flow and heat transfer in microchannel heat sink with offset ribs on sidewalls", Applied Thermal Engineering, v. 92, pp.32-41. https://doi.org/10.1016/j.applthermaleng.2015.09.071.

[25] Chai, L., Xia, G.D. and Wang, H.S., (2016)., "Parametric study on thermal and hydraulic characteristics of laminar flow in microchannel heat sink with fan-shaped ribs on sidewalls–Part 1: Heat transfer", International Journal of Heat and Mass Transfer, v. 97, pp.1069-1080. https://doi.org/10.1016/j.ijheatmasstransfer.2016.02.077.

[26] Ali, N., Haque, I., Alam, T., Siddiqui, T.U., Ansari, M.A., Yadav, J., Srivastava, S., Cuce, E., Ashraf, I. and Dobrotă, D., (2025)., "Numerical investigation on heat transfer and flow mechanism in microchannel heat sink having V shape ribs", Case Studies in Thermal Engineering, v. 65, p.105684. https://doi.org/10.1016/j.csite.2024.105684.

[27] Ahmed, H.E., Ahmed, M.I., (2015)., "Optimum thermal design of triangular, trapezoidal and rectangular grooved microchannel heat sinks", International Communications in Heat and Mass Transfer, v. 66, pp. 47-57. https://doi.org/10.1016/j.icheatmasstransfer.2015.05. 009.

[28] Chai, L., Xia, G., Wang, L., Zhou, M. and Cui, Z., (2013)., "Heat transfer enhancement in microchannel heat sinks with periodic expansion–constriction cross-sections", International Journal of Heat and Mass Transfer, v. 62, pp.741-751. https://doi.org/ 10.1016/j.ijheatmasstransfer.2013.03.045.

[29] Li, Y.F., Xia, G.D., Ma, D.D., Jia, Y.T. and Wang, J., (2016)., "Characteristics of laminar flow and heat transfer in microchannel heat sink with triangular cavities and rectangular ribs", International Journal of Heat and Mass Transfer, v. 98, pp.17-28. https://doi.org/ 10.1016/j.tca.2013.09.011.

[30] Ghani, I. A., Kamaruzaman, N., & Sidik, N. A. C., (2017)., "Heat transfer augmentation in a microchannel heat sink with sinusoidal cavities and rectangular ribs", International Journal of Heat and Mass Transfer, v.108, pp.1969-1981. https://doi.org/10.1016/ j.ijheatmasstransfer.2017.01.046.

[31] Wang, Y., Liu, J., Yang, K., Liu, J. and Wu, X., (2024)., "Performance and parameter optimization design of microchannel heat sink with different cavity and rib combinations", Case Studies in Thermal Engineering, v. 53, p.103843.

[32] Gönül, A., (2025)., Enhancement of heat transfer characteristics in wavy microchannel heat sinks with streamlined micropins within convergent-divergent flow passages, Applied Thermal Engineering, v. 258, p.124574. https://doi.org/10.1016/j.applthermaleng.2024. 124574.

[33] Kandlikar, S.G., Colin, S., Peles, Y., Garimella, S., Pease, R.F., Brandner, J.J. and Tuckerman, D.B., (2013)., "Heat transfer in microchannels—2012 status and research needs", Journal of Heat Transfer, 135(9), p.091001. https://doi.org/10.1115/1.4024354.

[34] Lee, Y.J., Lee, P.S. and Chou, S.K., (2009)., "Enhanced microchannel heat sinks using oblique fins", International Electronic Packaging Technical Conference and Exhibition, v. 43604, pp. 253-260. https://doi.org/10.1115/InterPACK2009-89059.

[35] Ghani, I.A., Sidik, N.A.C. and Kamaruzaman, N., (2017)., "Hydrothermal performance of microchannel heat sink: The effect of channel design", International Journal of Heat and Mass Transfer, v. 107, pp.21-44. https://doi.org/10.1016/j.ijheatmasstransfer.2016.11.031.

[36] Japar, W.M.A.A., Sidik, N.A.C. and Mat, S., (2018)., "A comprehensive study on heat transfer enhancement in microchannel heat sink with secondary channel", International Communications in Heat and Mass Transfer, v. 99, pp.62-81. https://doi.org/10.1016/ j.icheatmasstransfer.2018.10.005.

[37] Shi, X., Li, S., Mu, Y. and Yin, B., (2019)., "Geometry parameters optimization for a microchannel heat sink with secondary flow channel", International Communications in Heat and Mass Transfer, v. 104, pp.89-100. https://doi.org/10.1016/j.icheatmasstransfer. 2019.03.009.

[38] Bala Subrahmanyam, K. and Das, P., (2023)., "Numerical investigation of heat transfer enhancement in microchannel heat sink with fan cavities using secondary channels and ribs", Proceedings of the Institution of Mechanical Engineers, Part E: Journal of Process Mechanical Engineering, v. 237(5), pp.1783-1798. https://doi.org/10.1177/095440892 21127132.

[39] Bala Subrahmanyam, K., Das, P. and Ranjith Kumar, V., (2024)., "An overview of conjugate heat transfer augmentation methods for thermal management and recent advancements in microchannel heat sink overall performance", Proceedings of the Institution of Mechanical Engineers, Part E: Journal of Process Mechanical Engineering, p.09544089241253687. https://doi.org/10.1177/09544089241253687.

[40] Zhu, Q., Liu, X., Zeng, J., Zhao, H., He, W., Deng, H. and Chen, G., (2025)., "Numerical study of heat transfer and fluid flow in a symmetric wavy microchannel heat sink reinforced by slanted secondary channels", Case Studies in Thermal Engineering, v. 65, p.105605. https://doi.org/10.1016/j.csite.2024.105605.

[41] Kumar, V., Mondal, S., Datta, A. and Agrawal, A., (2024)., "A flow structure design based novel micro heatsink", Physics of Fluids, v. 36(7). https://doi.org/10.1063/5.0215512.

[42] Peng, J., (2025)., February, "Numerical study on hydraulic and heat transfer characteristics of diamond-shaped staggered rib microchannel heat sink", In Journal of Physics: Conference Series, v.2964, No.1, p.012021, IOP Publishing. DOI:10.1088/1742-6596/2964/1/012021.

[43] Faghri, A., (2012)., "Review and advances in heat pipe science and technology", Journal of heat transfer, v. 134(12), pp.123001. https://doi.org/10.1115/1.4007407.

[44] Jambunathan, K., Lai, E., Moss, M. and Button, B.L., (1992)., "A review of heat transfer data for single circular jet impingement", International journal of heat and fluid flow, v. 13(2), pp.106-115. https://doi.org/10.1016/0142-727X(92)90017-4.

[45] Kim, J., (2007)., "Spray cooling heat transfer: The state of the art", International Journal of Heat and Fluid Flow, v. 28(4), pp.753-767. https://doi.org/10.1016/j.ijheatfluidflow.2006.09.003.

[46] Mostafa. Y. T, El-Dosoky. M. F., M. Abdelgawad, Hassan. O., (2023)., "Numerical investigation of a hybrid double layer microchannel heat sink with jet impingement", International Journal of Thermofluids, v. 20, pp.100465. https://doi.org/10.1016/j.ijft. 2023.100465.

[47] Vamsi, B.V.S.R., Raveendiran, P. and Sastry, M.R.C., (2021)., "Experimental and numerical study of fluid flow and heat transfer in the impinging of inline round jets", Journal of Thermal Engineering, v. 11(1), pp.270-289.

[48] Chandratilleke, T.T., Jagannatha, D. and Narayanaswamy, R., (2009), December. "Performance analysis of a synthetic jet-microchannel hybrid heat sink for electronic cooling", In 2009 11th Electronics Packaging Technology Conference (pp. 630-635), IEEE. https://doi.org/10.1109/ EPTC.2009.5416472.

[49] Hoang, C.H., Tradat, M., Manaserh, Y., Ramakrisnan, B., Rangarajan, S., Hadad, Y., Schiffres, S. and Sammakia, B., (2020), October., "Liquid cooling utilizing a hybrid microchannel/multi-jet heat sink: A component level study of commercial product", In International Electronic Packaging Technical Conference and Exhibition (v. 84041, p. V001T08A008). American Society of Mechanical Engineers. https://doi.org/10.1115/ IPACK2020-2627.

[50] Song. Z., (2023)., "Effect of Heat Transfer Performance and Thermodynamic Analysis of Complex Structured Double-layer Microchannels Heat Sink" Highlights in Science, Engineering and Technology, v. 41, CDMMS-2023. https://doi.org/10.54097/hset.v41i. 6819.

[51] Yaghoobi, A. and Kharati-koopaee, M., (2021)., "Numerical investigation of fluid flow and heat transfer within multilayer wavy microchannels, Journal of Thermal Engineering, v. 10(3), pp.622-637.

[52] Ramesh, K.N., Sharma, T.K. and Rao, G., (2021)., "Latest advancements in heat transfer enhancement in the micro-channel heat sinks: a review", Archives of Computational Methods in Engineering, v. 28(4), pp.3135-3165.https://doi.org/10.1007/s11831-020-09495-1.

[53] Ghule, V.M., Pawar, A.A., Patil, L.N. And Javanjal, V.K., (2025)., "Numerical and experimental investigation of cross cut angle impact on heat transfer in microchannels", Sigma, v. 43(2), pp.463-486. https://doi.org/10.1016/j.applthermaleng.2024.124574.

[54] Liu, P., Sun, R., Hu, L. and Qiu, Y., (2024)., "Numerical study of heat transfer and entropy generation in ribbed microchannel with nanofluid and multiple jet impingement", Case Studies in Thermal Engineering, v. 62, p.105208. https://doi.org/10.1016/j.csite.2024. 105208.

[55] Kuppusamy, N.R., Mohammed, H.A. and Lim, C.W., (2013)., "Numerical investigation of trapezoidal grooved microchannel heat sink using nanofluids", Thermochimica acta, v. 573, pp.39-56. https://doi.org/10.1016/j.tca.2013.09.011.

[56] Bahiraei, M., Jamshid mofid, M. and Goodarzi, M., (2019)., "Efficacy of a hybrid nanofluid in a new microchannel heat sink equipped with both secondary channels and ribs", Journal of Molecular Liquids, v.273, pp.88-98. https://doi.org/10.1016/j.molliq. 2018.10.003.

[57] Sarafraz, M.M. and Arjomandi, M., (2018)., "Demonstration of plausible application of gallium nano-suspension in microchannel solar thermal receiver: experimental assessment of thermo-hydraulic performance of microchannel", International Communications in Heat and Mass Transfer, v. 94, pp.39-46. https://doi.org/10.1016/j.icheatmasstransfer. 2018.03. 013.

[58] Souby, M.M., Salman, M., Prabakaran, R. and Kim, S.C., (2023)., "Hydrothermal characteristics and irreversibility behavior of microchannel heat sink operated with hybrid nanofluids: A critical assessment", Case Studies in Thermal Engineering, v. 49, p.103387. https://doi.org/10.1016/j.csite.2023.103387.

[59] Souby, M.M., Bargal, M.H., Maher, H., Salman, M., Liu, J. and Kim, S.C., (2024)., "Numerical assessment of hydrothermal and entropy generation characteristics of graphene quantum dots nanofluid in a microchannel heat sink incorporating secondary channels and ribs", Case Studies in Thermal Engineering, v. 61, p.104894. https://doi.org/10.1016/ j.csite.2024.104894.

[60] Najafpour, A. and Rostami, M.H., (2025)., "Numerical analysis of thermal and hydrothermal characteristics of a heat sink with various fin configurations and ternary nanofluid composition", Case Studies in Thermal Engineering, v. 68, p.105928. https://doi.org/10.1016/ j.csite.2025.105928.

[61] Arshad, A., Ikhlaq, M., Saeed, M. and Imran, M., (2024)., "Numerical analysis of mono and hybrid nanofluids-cooled micro finned heat sink for electronics cooling-(Part-I) ", International Journal of Thermofluids, v. 23, p.100810. https://doi.org/10.1016/ j.ijft.2024.100810.

[62] Arshad, A., Ikhlaq, M., Saeed, M. and Imran, M., (2024)., "Numerical analysis of mono and hybrid nanofluids-cooled micro finned heat sink for electronics cooling-(Part-II) ". Thermal Science and Engineering Progress, v. 55, p.103005. https://doi.org/10.1016/ j.tsep.2024.103005.

[63] Veeraraghavan, G., Subramaniam, P. and Rajesh, M., (2025)., "Computational and experimental studies on the thermal performance of synthesized composite nanofluid in rectangular microchannel heat sink", Results in Engineering, v. 25, p.103687. https://doi.org/10.1016/j.rineng. 2024.103687.

[64] Chen, C.H. and Yaji, K., (2025)., "Topology optimization for microchannel heat sinks with nanofluids using an Eulerian-Eulerian approach", International Journal of Heat and Mass Transfer, v. 243, p.126870. https://doi.org/10.1016/j.ijheatmasstransfer.2025.126870.

[65] Kamsuwan, C., Wang, X., Seng, L.P., Xian, C.K., Piemjaiswang, R., Piumsomboon, P., Manatura, K., Kaewbumrung, M., Pratumwal, Y., Otarawanna, S. and Chalermsinsuwan, B., (2023)., "Enhancing performance of polymer-based microchannel heat exchanger with nanofluid: A computational fluid dynamics-artificial neural network approach", South African Journal of Chemical Engineering, v. 46(1), pp.361-375. https://doi.org/10.1016/ j.sajce.2023.09.001.

[66] Liao, C.C., Li, W.K. and Lin, H.E., (2025)., "Heat transfer enhancement in microchannel systems through geometric modification of vortex generators and nanofluid integration: A numerical study", Results in Engineering, v. 25, p.104138. https://doi.org/10.1016/ j.rineng.2025.104138.

[67] Suja, S.B., Islam, M.R. and Ahmed, Z.U., (2024), "Numerical investigation of thermal and hydraulic characteristics in porous pin fin heat sinks using single phase nanofluids", International Journal of Thermofluids, v. 22, p.100677. https://doi.org/10.1016/ j.ijft.2024.100677.

[68] Tuaima, A.N., Shkarah, A.J. and Salman, M.D., (2024), "The influence of micro-channel shape filled by nanofluid on heat transfer characteristics: Numerical and experimental study", Al-Qadisiyah J Eng Sci, v. 17, pp.029-37. https://doi.org/10.30772/qjes.2023. 143746.1039.

[69] Göksu, T.T., (2024), "Enhancing cooling efficiency: innovative geometric designs and mono-hybrid nanofluid applications in heat sinks", Case Studies in Thermal Engineering, v. 55, p.104096. https://doi.org/10.1016/j.csite.2024.104096.

[70] Chu, Y.M., Farooq, U., Mishra, N.K., Ahmad, Z., Zulfiqar, F., Yasmin, S. and Khan, S.A., (2023), "CFD analysis of hybrid nanofluid-based microchannel heat sink for electronic chips cooling: applications in nano-energy thermal devices", Case Studies in Thermal Engineering, v. 44, p.102818. https://doi.org/10.1016/j.csite.2023.102818.

[71] Qu, C., Zheng, J., Wu, S., Dai, R. and Zhang, J., (2023), "Multi-objective optimization of thermal and hydraulic performance with various concentrations of hybrid Fe3O4/graphene nanofluids in a microchannel heat sink", Case Studies in Thermal Engineering, v. 45, p.102963. https://doi.org/10.1016/j.csite.2023.102963.

[72] Nabi, H., Gholinia, M. and Ganji, D.D., (2023), "Employing the (SWCNTs-MWCNTs)/H2O nanofluid and topology structures on the microchannel heatsink for energy storage: A thermal case study", Case Studies in Thermal Engineering, v. 42, p.102697. https://doi.org/10.1016/j.csite.2023.102697.

[73] Nimmagadda, R. and Venkatasubbaiah, K., (2015), "Conjugate heat transfer analysis of micro-channel using novel hybrid nanofluids (Al2O3+ Ag/Water) ", European Journal of Mechanics-B/Fluids, v. 52, pp.19-27. https://doi.org/10.1016/j.euromechflu.2015.01.007.

[74] Takabi, B. and Shokouhmand, H., (2015), "Effects of Al 2 O 3–Cu/water hybrid nanofluid on heat transfer and flow characteristics in turbulent regime", International Journal of Modern Physics C, v. 26(04), p.1550047. https://doi.org/10.1142/S0129183115500473.

[75] Suresh, S., Venkitaraj, K.P., Selvakumar, P. and Chandrasekar, M., (2011), "Synthesis of Al2O3–Cu/water hybrid nanofluids using two step method and its thermo physical properties", Colloids and Surfaces A: Physicochemical and Engineering Aspects, v. 388(1-3), pp.41-48. https://doi.org/10.1016/j.colsurfa.2011.08.005.

[76] Sundar, L.S., Singh, M.K. and Sousa, A.C., (2014), Enhanced heat transfer and friction factor of MWCNT–Fe3O4/water hybrid nanofluids, International Communications in Heat and Mass Transfer, v. 52, pp.73-83. https://doi.org/10.1016/j.icheatmasstransfer. 2014.01. 012.

[77] Yarmand, H., Gharehkhani, S., Ahmadi, G., Shirazi, S.F.S., Baradaran, S., Montazer, E., Zubir, M.N.M., Alehashem, M.S., Kazi, S.N. and Dahari, M., (2015), "Graphene nanoplatelets–silver hybrid nanofluids for enhanced heat transfer", Energy conversion and management, v. 100, pp.419-428. https://doi.org/10.1016/j.enconman.2015.05.023.

[78] Megatif, L., Ghozatloo, A., Arimi, A. and Shariati-Niasar, M., (2016), "Investigation of laminar convective heat transfer of a novel TiO2–carbon nanotube hybrid water-based nanofluid", Experimental Heat Transfer, v. 29(1), pp.124-138. https://doi.org/10.1080/ 08916152.2014.973974.

[79] Madhesh, D. and Kalaiselvam, S., (2014), "Experimental analysis of hybrid nanofluid as a coolant", Procedia engineering, v. 97, pp.1667-1675. https://doi.org/10.1016/j.proeng.2014.12.317.

[80] Jani, M.N.S. and Saeid, N., (2024)., "Thermal stress analysis in pin fin microchannel heat sink", Journal of Thermal Engineering, v. 10(2), pp.273-285. https://doi.org/10.18186/thermal.1448547.

[81] Alihosseini, Y., Oghabneshin, Y., Bari, A.R., Moslemi, S., Targhi, M.Z., Guo, W. and Mashhadian, A., (2024), "Oblique microchannel merged with circle micro pin-fin as a novel hybrid heat sink for cooling of electronic devices", Case Studies in Thermal Engineering, v. 53, p.103888. https://doi.org/10.1016/j.csite.2023.103888.

[82] Raafat, A., Alteneiji, M., Kamra, M. and Al Nuaimi, S., (2025)., "Hydrothermal performance of microchannel heat sink integrating pin fins based on triply periodic minimal surfaces", Case Studies in Thermal Engineering, v. 66, p.105773. https://doi.org/10.1016/j.csite.2025.105773.

[83] Xie, G., Shen, H. and Wang, C.C., (2015)., "Parametric study on thermal performance of microchannel heat sinks with internal vertical Y-shaped bifurcations", International journal of heat and mass transfer, v. 90, pp.948-958. http://dx.doi.org/10.1016/j. ijheatmasstransfer. 2015.07.034.

[84] Xia, G., Ma, D., Zhai, Y., Li, Y., Liu, R. and Du, M., (2015)., "Experimental and numerical study of fluid flow and heat transfer characteristics in microchannel heat sink with complex structure" Energy Conversion and Management, v. 105, pp.848-857. https://doi.org/10.1016/j.enconman.2015.08.042.

[85] Kuppusamy, N.R., Saidur, R., Ghazali, N.N.N. and Mohammed, H.A., (2014)., "Numerical study of thermal enhancement in micro channel heat sink with secondary flow", International journal of heat and mass transfer, v. 78, pp.216-223. http://dx.doi.org/ 10.1016/ j.ijheatmasstransfer.2014.06.072.

[86] Vinodhan, V.L. and Rajan, K.S., (2014)., "Computational analysis of new microchannel heat sink configurations", Energy Conversion and Management, v. 86, pp.595-604. http://dx.doi.org/ 10.1016/j.enconman.2014.06.038.

[87] Sui, Y., Teo, C.J., Lee, P.S., Chew, Y.T. and Shu, C., (2010)., "Fluid flow and heat transfer in wavy microchannels. International Journal of Heat and Mass Transfer, v. 53(13-14), pp.2760-2772. https://doi.org/10.1016/j.ijheatmasstransfer.2010.02.022.

[88] Mohammed, H.A., Gunnasegaran, P. and Shuaib, N.H., (2011)., "Numerical simulation of heat transfer enhancement in wavy microchannel heat sink", International Communications in Heat and Mass Transfer, v. 38(1), pp.63-68. https://doi.org/10.1016/j.icheatmasstransfer. 2010.09.012.

[89] Deng, D., Wan, W., Tang, Y., Shao, H. and Huang, Y., (2015)., "Experimental and numerical study of thermal enhancement in reentrant copper microchannels", International Journal of Heat and Mass Transfer, v. 91, pp.656-670. https://doi.org/10.1016/ j.ijheatmasstransfer.2015.08.025.

[90] Lee, Y.J., Lee, P.S. and Chou, S.K., (2012), "Enhanced thermal transport in microchannel using oblique fins", v. 134(10):101901. https://doi.org/10.1115/1.4006843.

[91] Fan, Y., Lee, P.S., Jin, L.W. and Chua, B.W., (2013)., "A simulation and experimental study of fluid flow and heat transfer on cylindrical oblique-finned heat sink", International journal of heat and mass transfer, v. 61, pp.62-72. https://doi.org/10.1016/ j.ijheatmasstransfer.2013.01.075.

[92] Tullius, J.F., Vajtai, R. and Bayazitoglu, Y., (2011)., "A review of cooling in microchannels, Heat Transfer Engineering, v. 32(7-8), pp.527-541. https://doi.org/10.1080/01457632.2010.506390.

[93] Incropera, F.P., (1999)., "Liquid cooling of electronic devices by single-phase convection"., pp. 262–263. https://lccn.loc.gov/98053676.

[94] Gao, Q., Lizarazo-Adarme, J., Paul, B.K. and Haapala, K.R., (2016)., "An economic and environmental assessment model for microchannel device manufacturing: part 1–Methodology", Journal of cleaner production, v. 120, pp.135-145. https://doi.org/10.1016/ j.jclepro.2015.04.142.

[95] Gao, Q., Lizarazo-Adarme, J., Paul, B.K. and Haapala, K.R., (2016)., "An economic and environmental assessment model for microchannel device manufacturing: part 2–Application", Journal of Cleaner Production, v. 120, pp.146-156. https://doi.org/10.1016/ j.jclepro.2015.04.141.

[96] Bartlett, N.W. and Wood, R.J., (2016)., "Comparative analysis of fabrication methods for achieving rounded microchannels in PDMS", Journal of Micromechanics and Microengineering, v. 26(11), p.115013. Doi: 10.1088/0960-1317/26/11/115013

[97] Nicholas. W, Bartlett and Robert. J. Wood., (2016)., "Comparative analysis of fabrication methods for achieving rounded microchannels in PDMS", 0–10. Doi:10.1088/0960-1317/26/11/115013.
[98] Wilson, M.A., Recknagle, K. and Brooks, K., (2005)., "Design and development of a low-cost, high temperature silicon carbide micro-channel recuperator", v. 46997, pp. 1029-1034. https://doi.org/10.1115/GT2005-69143.
[99] Chrysler, G.M. and Prasher, R., Intel Corp, (2006)., "Integrated micro channels and manifold/plenum using separate silicon or low-cost polycrystalline silicon", U.S. Patent 6,992,382.
[100] Collins, I.L., Weibel, J.A., Pan, L. and Garimella, S.V., (2018)., "Evaluation of additively manufactured microchannel heat sinks. IEEE Transactions on Components", Packaging and Manufacturing Technology, v. 9(3), pp.446-457. https://doi.org/10.1109/TCPMT. 2018. 2866972.